

UNIVERSITÀ DEGLI STUDI DI PADOVA

DIPARTIMENTO DI INGEGNERIA INDUSTRIALE
CORSO DI LAUREA MAGISTRALE IN INGEGNERIA CHIMICA E DEI
PROCESSI INDUSTRIALI

**Tesi di Laurea Magistrale in
Ingegneria Chimica e dei Processi Industriali**

**A SUPERCRITICAL FLUID EXTRACTION PROCESS
TO OBTAIN VALUABLE COMPOUNDS
FROM *ERUCA SATIVA* LEAVES**

Relatore: Prof. Alberto Bertucco

Correlatore: Ing. Miriam Solana Ciprés

Laureando: SHEFQET MIROFCI

ANNO ACCADEMICO: 2013-2014

Abstract

Supercritical carbon dioxide extraction of glucosinolates, flavonoids and lipids from leaves of rocket salad (*Eruca sativa*) is presented in this work. SC-CO₂ extraction has been compared with Soxhlet extraction method. In the case of SC-CO₂ method, extractions with pure CO₂ and co-solvents have been carried out. Three different co-solvents have been compared: water, ethanol and methanol. First, SC-CO₂ extraction has been performed using ethanol as co-solvent. The effect of the different variables that affect the process has been studied, obtaining the best results at 300 bar, 65°C, CO₂ flow rate of 0.3 kg/h and ethanol dosage of 0.5 mL/min. The effect of a mechanical pre-treatment on the yield of the extraction has also been reported. Then, SC-CO₂ extraction has been performed using water as co-solvent. The optimum values of the water dosage and of the extraction temperature have been obtained at 0.4 mL/min and 65°C, while pressure does not affect significantly the extraction yield. When ethanol, methanol and water as co-solvents at the same extraction conditions have been compared, the highest yield has been obtained with water. The extracts have been analyzed and the results show that flavonoids and glucosinolates have been mainly extracted using water as co-solvent, while lipids have been extracted using pure SC-CO₂. A conceptual design of an industrial scale application of the process has been proposed, using the software Aspen Plus 7.3 for the simulation. The lowest production cost was found at extraction conditions of 250 bar and 65°C and separation pressure of 72 bar. An analysis of the profitability of the process has also been performed.

Riassunto

L'estrazione è stata per trent'anni il maggior impiego dei fluidi supercritici. Una sostanza pura è considerata nello stato supercritico se la sua temperatura e la sua pressione sono superiori a quelle critiche. In queste condizioni le proprietà fisiche della sostanza assumono caratteristiche uniche, ibride tra quelle in fase gas e quelle in fase vapore. In particolare i valori di alta diffusività, bassa tensione superficiale e bassa viscosità li accomunano ai gas, mentre i valori della densità li accomunano ai liquidi. A temperatura costante, cambiando la pressione si cambia la densità, che a sua volta porta al cambiamento di proprietà come la capacità del solvente, la viscosità e la diffusività, e la costante dielettrica. Queste caratteristiche permettono ai fluidi supercritici di essere utilizzati come solventi nell'estrazione di sostanze da prodotti naturali: essi possono penetrare la sostanza biologica ed offrono un potere solvente che può essere aggiustato in modo da solubilizzare ed estrarre il componente chimico di interesse. Il fluido supercritico più usato è l'anidride carbonica. Questa unisce ai già citati vantaggi dei fluidi supercritici, il fatto di presentare condizioni critiche facilmente raggiungibili e di essere non infiammabile, non tossica, economica. Inoltre l'anidride carbonica può essere completamente recuperata dopo l'estrazione per semplice depressurizzazione, non lasciando alcuna traccia nell'estratto. Queste caratteristiche la rendono ideale come solvente da usare nell'industria alimentare.

In questo lavoro si è utilizzata l'anidride carbonica supercritica per estrarre componenti chimici ad alto valore aggiunto da foglie di rucola (*Eruca sativa*). Fonti di letteratura mostrano che le foglie di rucola contengono glucosinolati e flavonoidi, mentre i semi sono ricchi di acidi grassi. I glucosinolati sono metaboliti secondari che si trovano all'interno dei vacuoli, tipici delle piante della famiglia delle (*Brassicaceae*). È confermato che un'assunzione regolare di questi composti è in grado di limitare la probabilità di insorgere di malattie cardiovascolari, in particolare la glucorafanina è nota per essere la sostanza che più di ogni altra stimola il fegato a produrre disintossicanti che impediscono l'insorgere di cancro al petto e al colon. Pure i flavonoidi (composti polifenolici) sono metaboliti secondari presenti nei tessuti delle foglie noti per avere proprietà antiossidanti e anticancerogene.

In questo lavoro si estraggono glucosinolati, flavonoidi e acidi grassi da foglie di rucola usando la tecnica dell'estrazione con CO₂ supercritica. In letteratura ci sono articoli di estrazione supercritica di glucosinolati dalla pianta di colza e di flavonoidi da foglie di Ginkgo utilizzando l'etanolo come co-solvente. Acidi grassi sono invece stati estratti in letteratura da foglie di broccoli (appartenenti alla stessa famiglia della rucola, *Brassicaceae*), utilizzando l'anidride carbonica pura o addizionata con metanolo per estrarre gli acidi grassi più polari.

L'estrazione è stata effettuata usando un impianto di estrazione supercritica da laboratorio. Le foglie di rucola prima dell'estrazione hanno subito un pre-trattamento di disidratazione (liofilizzazione) per eliminare l'acqua che potrebbe interferire con l'estrazione. Si sono sostenute diverse condizioni di temperatura (da 45 a 75 °C) e pressione (da 150 a 300 bar) di estrazione al fine di individuare i valori ottimali. Gli estratti ottenuti sono stati poi analizzati per investigare l'influenza delle condizioni di estrazione sulla composizione dell'estratto. HPLC e NMR sono state le due tecniche utilizzate per le analisi della composizione.

La resa dell'estrazione supercritica è stata paragonata con quella ottenuta con l'estrazione Soxhlet, mostrando che la prima oltre a richiedere tempo e temperature inferiori può avere anche rese simili.

Le condizioni dell'estrazione sono state ottimizzate utilizzando l'etanolo come co-solvente. Si è visto che un aumento della portata di CO₂ porta ad una diminuzione della resa, 0,3 kg/h si è scelto come portata ottimale. Un trattamento meccanico per ridurre le dimensioni delle particelle è stato effettuato ottenendo chiari miglioramenti nella resa, dovuti all'aumento dell'area interfacciale, alla rottura meccanica delle pareti cellulari e alla diminuzione del diametro delle particelle solide che favorisce la diffusione. Si è osservato che la portata di etanolo ha un valore ottimale (0,5 mL/min) al di sopra del quale un aumento della concentrazione di etanolo non porta ad un aumento della resa. Un aumento della pressione comporta invece un aumento della resa (miglior risultato a 300 bar). Analogamente, a temperature elevate si sono osservate rese elevate. Accanto all'etanolo anche l'acqua è stata utilizzata come co-solvente, e si è trovato che la portata ottimale di acqua è di 0,4 mL/min. Si è osservato che la temperatura è la variabile che maggiormente influenza la resa dell'estrazione, riscontrando notevoli incrementi nei valori della resa quando si passa da 45 °C a 65 °C. Al contrario della temperatura si è visto che l'influenza della pressione, pur portando ad aumenti del valore della resa all'aumentare della pressione, risulta meno marcata e non ben distinguibile. Nelle stesse condizioni di estrazione (300 bar, 45°C, 7% di co-solvente) tre diversi co-solventi sono stati impiegati: etanolo, metanolo e acqua. Le rese ottenute con etanolo e metanolo sono simili (5,54 e 5,56 %), mentre quella con l'acqua risulta essere di molto superiore (21 %).

Le analisi degli estratti hanno mostrato l'influenza delle condizioni di estrazione sulla composizione dell'estratto. I glucosinolati sono stati estratti utilizzando l'acqua come co-solvente mentre non si sono riscontrati negli estratti ottenuti con con l'etanolo o il metanolo. La quantità maggiore di glucosinolati è stata ottenuta a 300 bar e con 0,4 mL/min di acqua. Curiosamente la quantità di glucosinolati ottenuti con la rucola non filtrata risulta maggiore di quella ottenuta con quella filtrata. I componenti principali sono stati glucorafanina e DMB-glucosinolato. Anche i flavonoidi sono stati estratti utilizzando l'acqua come co-solvente. La concentrazione maggiore di flavonoidi è stata ottenuta 0,4 mL/min di acqua, in particolare risulta essere influenzata dalla temperatura presentando la massima quantità alla massima

temperatura utilizzata (75 °C). Principalmente i flavonoidi estratti sono stati Quercetina e suoi derivati. Flavonoidi e glucosinolati sono stati estratti utilizzando la CO₂ supercritica (addizionata da acqua come co-solvente) mentre sono presenti solo in tracce negli estratti ottenuti con l'estrazione Soxhlet. Negli estratti ottenuti utilizzando l'acqua come co-solvente non vi erano tracce di acidi grassi, che invece sono stati estratti utilizzando solamente l'anidride carbonica supercritica pura. Gli estratti ottenuti erano ricchi in acidi grassi insaturi.

In questo lavoro si è voluto proporre una progettazione concettuale di uno scale up industriale dell'impianto di estrazione supercritica di laboratorio. Il software Aspen Plus V7.3 è stato utilizzato per tale scopo. Il processo produce estratto di rucola a partire da rucola, acqua e anidride carbonica, ed è principalmente costituito da un sistema di estrazione e uno di separazione. Il sistema di estrazione è costituito da due estrattori in serie che permettono di operare l'estrazione supercritica in modo semi-continuo, quello di separazione è costituito da un'unità per la separazione e il recupero dell'anidride carbonica, e da un'unità di essiccazione dell'estratto per eliminare e recuperare l'acqua utilizzata come co-solvente.

Una unità di calcolo è stata implementata per calcolare il costo di produzione per ottenere una portata di prodotto di 30 kg/h. L'influenza della temperatura di estrazione e della pressione di estrazione sul costo di produzione è stata analizzata. I valori operativi ottimali per l'estrazione si sono trovati essere 300 bar, e 65°C. Si è inoltre osservato che il costo di produzione tende a diminuire all'aumentare della pressione di separazione, fino al valore limite costituito dalla pressione critica. Un valore ottimale si è trovato per la portata di ricircolo di anidride carbonica di circa 30000 kg/h. Per le condizioni ottimali si sono poi calcolati i costi fissi dell'impianto. Si è osservato che i costi fissi annualizzati contribuiscono solo per il 10% al costo totale del prodotto. Il costo delle materie prime risulta essere quello che maggiormente influisce sul costo totale del prodotto (50%).

Infine è stata effettuata un'analisi sulla redditività del processo. Come base di calcolo si è considerato una vita utile dell'impianto di 10 anni con un ammortamento dei costi di impianto di 7 anni. Si è osservato che con un tasso di interesse pari al 10 % per avere un valore attuale netto positivo, il prezzo di vendita dell'estratto deve essere superiore a 29.8 \$/kg.

Table of contents

CHAPTER 1.....	3
1.1 Supercritical fluids and their solvent power.....	3
1.1.1 Supercritical carbon dioxide.....	6
1.2 Literature review on <i>Eruca sativa</i> composition.....	8
1.2.1 Glucosinolates.....	9
1.2.2 Polyphenols.....	12
1.2.3 Fatty Acids.....	14
1.3 Literature review on supercritical CO ₂ extraction of glucosinolates, flavonoids and fatty acids from rocket salad.....	16
1.3.1 Supercritical CO ₂ extraction of glucosinolates.....	16
1.3.2 Supercritical CO ₂ extraction of phenolic compounds (flavonoids).....	17
1.3.3 Supercritical CO ₂ extraction of lipids.....	17
CHAPTER 2.....	19
2.1 Pre-treatment: Lyophilization of the leaves.....	19
2.2 Supercritical CO ₂ extraction process.....	22
2.3 Soxhlet extraction.....	27
2.4 Analysis of the extract.....	28
2.4.1 HPLC – MS.....	28
2.4.2 NMR.....	30
CHAPTER 3.....	33
3.1 Comparison of SCF extraction with Soxhlet extraction.....	33
3.2 Optimization of the extraction parameters using ethanol as co-solvent.....	34
3.2.1 Effect of CO ₂ flow rate on the yield of the extraction.....	34
3.2.2 Optimization of the ethanol dosage.....	36
3.2.3 Effect of the pre-treatment on the yield of the extraction.....	38
3.2.4 Optimization of the temperature on the extraction process.....	39
3.2.5 Optimization of the pressure on the extraction process.....	40
3.3 Optimization of the extraction parameters using water as co-solvent.....	41
3.3.1 Optimization of the water dosage.....	42
3.3.2 Optimization of the temperature on the extraction process.....	42
3.3.3 Optimization of the pressure on the extraction process.....	43

3.4 Comparison between three different co-solvents	44
3.5 Effect of the extraction conditions on the <i>Eruca sativa</i> extract composition	46
3.5.1 Glucosinolates	46
3.5.2 Phenols	49
3.5.3 Lipids.....	53
CHAPTER 4.....	55
4.1 Simulation model	55
4.1.1 Aspen Plus.....	57
4.2 Economical analysis of the process.....	62
References	75

Preface

Rocket salad (*Eruca sativa*) is a vegetable herb highly consumed in Italy as a salad ingredient. Literature overview reveals that it contains valuable health-promoting compounds. Glucosinolates and flavonoids are present in the leaves while seeds are rich in fatty acids. All these compounds have gained importance in recent years because of their healthy properties. Glucosinolates are associated with lower risk of the presence of cancer and cardiovascular disease while flavonoids are powerful antioxidants.

The aim of this thesis is to extract these compounds by supercritical fluid technology. Usually they are extracted with solvent extraction, methanol and ethanol being the most commonly used solvents. However they require high temperatures that can lead to the degradation of plant tissues losing these valuable compounds. Moreover, solvent extraction requires long residence time. In addition there are lots of legal restrictions in using these two solvents for food applications.

Supercritical fluid extraction seems to be appropriate for this extraction as it is fast and mostly operated at low temperatures. Moreover the solvent can be easily be separated from the extract by simple depressurization.

In this work carbon dioxide is used as supercritical solvent and its solubility power is modified by adding a suitable co-solvent to extract glucosinolates, flavonoids and fatty acids. A series of experiments have been carried out in order to find also the optimum extraction parameters including pressure, temperature, co-solvent concentration and carbon dioxide flow rate.

In Chapter 1 an overview on the supercritical fluid extraction and a literature review on the most valuable compounds of rocket salad and their extraction, is reported. In Chapter 2 the materials and the methods used during the experiments are reported. In Chapter 3 are shown the results of the experimental part and a discussion on the results are shown. In Chapter 4 a conceptual design of a possible industrial scale application is shown. Aspen plus software has been used for this purpose. Furthermore an economic feasibility analysis for this process is reported.

Finally, a conclusion part with the final results is reported.

CHAPTER 1

Introduction

Supercritical fluids are substances at pressures and temperatures above their critical values. For more than thirty years extraction using supercritical carbon dioxide has been the most widespread application of supercritical fluids. For various reasons, such as the solubility of the substances and the low effort required to separate the solvent after the extraction, supercritical fluids had their first application in the food industry. In this work supercritical carbon dioxide was used to extract valuable chemical compounds such as glucosinolates, polyphenols and fatty acids from leaves of rocket salad (*Eruca sativa*).

1.1 Supercritical fluids and their solvent power

A pure component is considered to be at the supercritical state when its temperature and its pressure are higher than the critical values. The standard phase diagram is shown in Figure 1.1, it represents the regions of temperature and pressure where the substance is present as solid, as liquid and as gas.

These phases are separated by equilibrium phase transition lines. The three phase boundaries meet at the triple point, where the three phases coexist. The diagram shows that the supercritical fluid region is apart from the three standard aggregate states.

Following the gas–liquid coexistence curve, both temperature and pressure increase. The liquid becomes less dense because of thermal expansion, and the gas becomes denser as pressure rises.

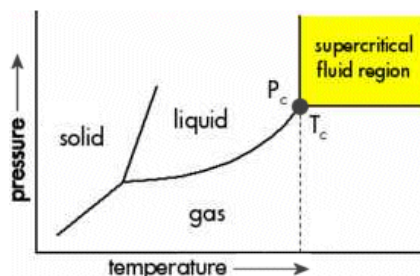


Figure 1.1 Generalized qualitative P-T phase diagram

At critical conditions of pressure and temperature, P_c and T_c respectively, the densities of the two phases becomes identical and there is no practically distinction between the gas and the liquid.

Above these conditions the substance can only be described as a supercritical fluid (Figure 1.2).

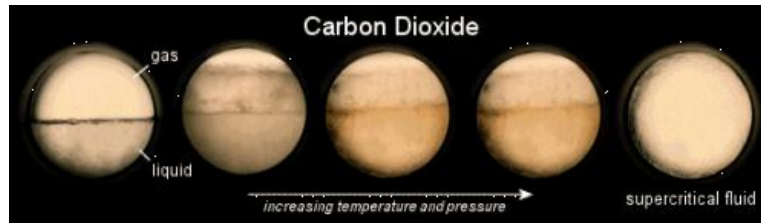


Figure 1.2 Supercritical Fluid

This transition can be better represented within the P-V diagram (Figure 1.3) (¹). In the P-T diagram heating up a saturated substance means moving up the boiling line, while in the P-V diagram it describes the isotherms rising and increasing the pressure on both the saturated liquid and the saturated vapor line.

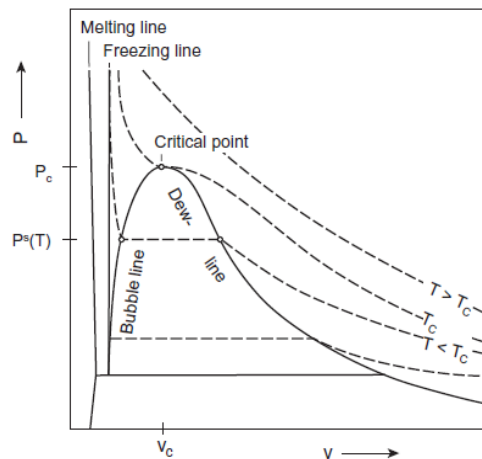


Figure 1.3 Qualitative P-V diagram.

For elevated conditions, the differences in density between the two lines decline and finally disappear approaching the critical conditions. It means that the intermolecular forces become equal and the thermal energy becomes equal.

The isotherm of the critical temperature touches the dew point line and the bubble point line at the critical point, exhibiting a saddle and a turning point. The critical point is also defined by the disappearance of the heat of vaporization.

Within the supercritical region there is no phase boundary between the gas and the liquid phases, meaning that there is a continuity in physical properties of the fluid between the gas and the liquid states.

The most important consequence is that supercritical fluids have properties which are a curious hybrid of those associated with liquids and gases. The viscosities and diffusivities are similar to those of the gases, while the density is closer to that of a liquid. A unique feature of supercritical fluids is their pressure-dependent density. If temperature is constant, density can

be adjusted by pressure from that of a vapor to that of a liquid with no discontinuity. Changing in density leads to simultaneous change of several other properties such as viscosity, solvent power, diffusivity and dielectric constant. Similar effects to that of the supercritical state can in some cases be achieved at near critical temperatures in the liquid state of a substance for $P > P_c$ and $T < T_c$. In this region, important changes and related properties such as solubility are observed with small changes in pressure. These characteristics make supercritical fluids very attractive as tunable process solvents. The combination of high solubility and low surface tension and low viscosity is especially attractive to extraction from solid raw materials where the target substances are deep inside pores.

Characteristic values for the gaseous, liquid, and supercritical state properties are listed in Table 1.1 (²). In the supercritical state, as previously said, liquid-like densities are approached, while viscosity is near that of normal gases and diffusivity is about two orders of magnitude higher than in typical liquids.

Table 1.1 :Characteristic values of gas, liquid and supercritical state

State of the fluid	Density (g/cm ³)	Diffusivity (cm ² /s)	Viscosity (g/cm/s)
<i>Gas</i> $p = 1 \text{ atm}, T = 15\text{--}30 \text{ }^\circ\text{C}$	$(0.6\text{--}2.0) \times 10^{-3}$	0.1–0.4	$(0.6\text{--}2.0) \times 10^{-4}$
<i>Liquid</i> $p = 1 \text{ atm}, T = 15\text{--}30 \text{ }^\circ\text{C}$	0.6–1.6	$(0.2\text{--}2.0) \times 10^{-5}$	$(0.2\text{--}3.0) \times 10^{-2}$
<i>Supercritical fluid</i> $p = p_c; T \approx T_c$	0.2–0.5	0.7×10^{-3}	$(1\text{--}3) \times 10^{-4}$
$p = 4p_c; T \approx T_c$	0.4–0.9	0.2×10^{-3}	$(3\text{--}9) \times 10^{-4}$

Certainly, the most important tunable property of a supercritical fluid is its solvent power, that makes it really suitable in processes where reduction of pressure and associated expansion of the solvent is an efficient method for recovering the products.

Besides the pressure effect, the solvent power of supercritical fluids depends on the molecule, its size and structure. Polarity is the main issue and not all substances exhibit the same solubility in compressed gases. Since in many cases the solvent power of the supercritical fluid is not enough (even at elevated pressure), co-solvents can be added to increase the polarity. In this way the polarity of the solvent can be manipulated to increase the solubility of the desired compound with supercritical CO₂, the two most typical co-solvents are ethanol and water. Both of them shift the polarity of the system and enable the extraction of polar components. The concentration and selection of the co-solvent depends on the substances to be extracted. Usually the amount of added co-solvent should not exceed 10 wt %, otherwise each of these solvents can be used on his own (¹).

The most popular fluids used at supercritical conditions are carbon dioxide and water. Since they are non-toxic and nonflammable, they are essentially environmentally benign solvents

that can be used, even for food processing, without significant regulation. In addition, they are two of the most inexpensive solvents available commercially (¹).

1.1.1 Supercritical carbon dioxide

While supercritical fluids in general exhibit interesting physical properties, there is a specific interest upon carbon dioxide due to its “easily” accessible supercritical state and its “green” properties.

In Figure 1.4 the critical points of some fluids are represented, which have already been utilized in technical plants using supercritical fluids (H₂O, CO₂, C₂H₄). Also chemically similar fluids are compared, for example by their bonding (C₂H₂, C₂H₄, C₂H₆), or by their molecular weights (C₂H₆, C₃H₈, C₄H₁₀, C₅H₁₂).

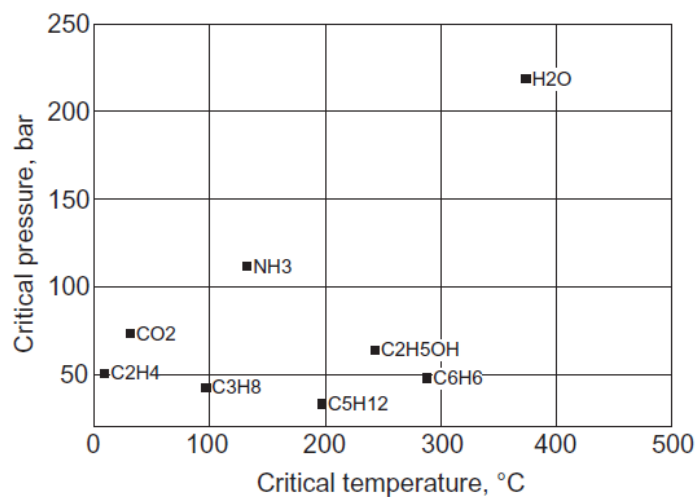


Figure 1.4: Critical points of some fluids

The critical point of carbon dioxide is at 7.38 MPa at 31.1 °C (³), so that means the supercritical regime is readily accessible compare to water. Its critical point is higher than analogous alkane. Carbon dioxide’s higher critical pressure is one result of the effect that its strong quadrupole moment exerts on its physical properties. Carbon dioxide is non-flammable, a significant safety advantage in using it as a solvent. The TLV (threshold limit value for airborne concentration at 25 °C to which it is believed that nearly all workers may be repeatedly exposed day after day without adverse effects) is 5000 ppm (⁴), rendering it less toxic than other organic solvents (acetone has a TLV of 750 ppm, chloroform is 10 ppm, pentane is 600 ppm (⁵)). Carbon dioxide is a greenhouse gas, but it is also a naturally abundant material that can be theoretically extracted from the atmosphere. However, most of carbon dioxide employed in processes is collected as a by-product of other processes as that of ammonia production or collected from natural sources. Carbon dioxide presents also safety disadvantages. Using it in a process certainly requires high pressure equipment, due to its high

vapour pressure at room temperature. This can be a potential safety hazard relative to the same process operating at atmospheric pressure.

Carbon dioxide can solubilise apolar components. Substances which have low molecule weight, such as alcohols, ketones, aldehydes and esters, are the basis for flavours and are well soluble in supercritical CO₂. Less soluble substances with higher molecular weight, are amino acids, proteins and carbohydrates (which are related to functionality). The solubility in supercritical CO₂ can be manipulated adding polar co-solvents such as ethanol, methanol or water.

Increasing attention to environmentally friendly production, and constantly increasing demands on product quality have forced the World Health Organization and the European Union to publish guidelines for solvents in food production (¹). Carbon dioxide is harmless solvent, which represents an advantage compared to traditional solvent extraction.

One further advantage of using supercritical carbon dioxide is the low process temperature, about 40 °C, at which extraction can be performed. This is specifically appropriate for food applications where increasing temperature can damage the thermo-sensible substances.

Up to the end of 2004 approximately 90 production plants have been installed, which use supercritical carbon dioxide.

Table 1.2 shows the distribution of industrial scale plants using supercritical fluids in the world.

Table 1.2 : Distribution of industrial scale SFE plants

Region	Number of installed SFE plants
Europe	45
Americas	5
Japan	17
China	9
Korea	3
India	3
Australia, New Zeland	3
Africa	1

Extraction with SC-CO₂ has been established for different applications, depending on their target. Two are the main targets. The first one is extraction to remove a substance to refine a raffinate, which is far larger in volume. This is the case of decaffeination of tea and coffee or the defatting of cacao.

The second one is extraction to obtain the extract as desired product. This is the case of the extraction of spices or fruit flavors or the extraction of milk products or fish oil components.

1.2 Literature review on *Eruca sativa* composition

Eruca sativa (in English “rocket salad”, in Italian “rucola”) is a vegetable herb of the family of *Brassicaceae*. It is native to the Mediterranean region and it is really popular among Middle Eastern and Europeans populations for its particular taste and flavour. The main species of rucola known and cultivated are *Eruca* and *Diplotaxis*. The latter is generally characterised by a more pungent taste. Italy is an important producer and especially the region of Veneto in the north-east.

In the Mediterranean area rocket salad has been consumed as salad since Roman times because of its nutritional property and especially because of its traditional benign effect on human health. In Southern Europe and in the Middle East rocket leaves have been used as digestion-aid, against eye infection and as deodorant and for cosmetic uses also as aphrodisiac⁽⁶⁾. In the Middle East also rocket salad seeds have also been used to produce an appreciated nutritional oil.



Figure 1.5: Leaf of Rucola

This ancient knowledge has been confirmed in recent years. Plants belonging to *Brassicaceae* family has gained greater importance because they possess diversified medicinal and therapeutic properties. Various authors have studied the health promoting effects of the chemical compounds of the members of *Brassicaceae* and especially that of rocket salad. In literature the gastric anti-ulceric activity of the rocket salad is reported⁽⁷⁾. Moreover, a mechanism how isothiocyanates protects the organism against colon-rectal cancer⁽⁸⁾ and the hepatoprotective activity of members of *Brassicaceae* have been studied⁽⁹⁾.

Generally, we can say that members of this family of vegetables are important for their content of generalist (vitamin C, carotenes and phenolic) specific (glucosinolates) health promoting compounds.⁽¹⁰⁾

Focusing on the *Eruca sativa* leaves, there are many articles in the literature that report the most valuable compounds of rocket salad. The main categories are glucosinolates and flavonoids, which are described below.

1.2.1 Glucosinolates

Glucosinolates are nitrogen- and sulfur- containing secondary metabolites that are limited to species of the order of *Capparales*, which includes broccoli, rape and salad such as *Eruca sativa*. Glucosinolates are also known as (z)-N-hydroximiniosulfate esters. They consist of a common glycone group and a variable aglycone side chain R derived from amino acids (usually methionine, phenylalanine, tyrosine and tryptophan (Figure 1.6)).

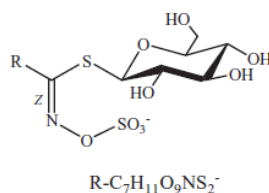


Figure 1.6 :General structure of glucosinolates

Extensive glucosinolate side chain modification and amino acid elongation are together responsible for the chemical diversity of more than 120 reported glucosinolate structures, which are classified as aliphatic, aromatic, *w*-methylthioalkyl and heterocyclic according to the type of side chain. These hydrophilic, stable compounds are normally situated in vacuoles of plant tissues. A damage to the tissue causing loss of cellular integrity initiates glucosinolate breakdown by hydrolysis of the glucosidic bond catalyzed by myrosinase. Myrosinases are specific β -thioglucosidases localized in idioblasts (myrosin cells). Thus, plant injury activates the glucosinolate-myrosinase system, leading to the rapid generation of unstable thiohydroximate-*O* sulfate intermediates. The consequent spontaneous rearrangement yields a variety of bioactive products which include isothiocyanates, thiocyanates, nitriles, oxazolidine-2, thiones or epithioalkanes. The final composition depends on chemical conditions such as pH, available ferrous ions and presence of protein interacting with myrosinase. Figure 1.7 refers not to rocket salad but to *Arabidopsis thaliana*, another plant of the same family that presents the glucosinolate – myrosinase system better explains this sequence. ⁽¹¹⁾

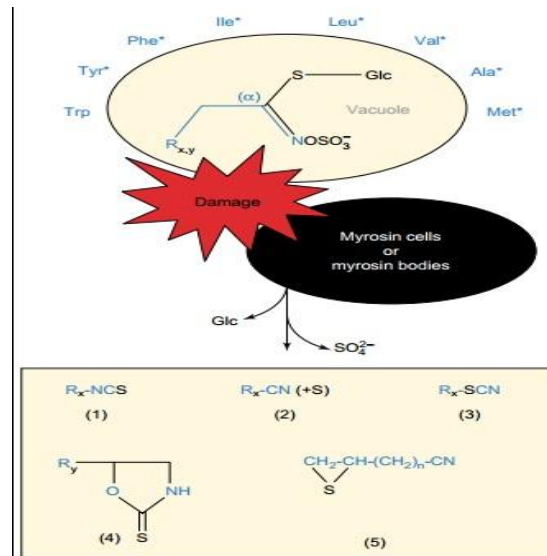


Figure 1.7: Glucosinolate-myrosinase system. Upon plant injury, glucosinolate released from vacuoles are hydrolyzed and the aglucone intermediate rearrange to form (1) Isothiocyanates at pH 5-8; (2) nitriles and elemental sulfur if guided by ethiospecific protein or at pH 2-5 in presence of Fe ions; (3) thiocyanates at pH >8; (4) oxazolidine-2-thiones if a hydroxyl function is present on carbon 3 of the glucosinolate; (5) epithionitriles if a terminal double bond captures elemental sulfur released during nitriles formation.

These degradation products of glucosinolates have an important role in plant defense against herbivores and pathogens because of their biocidal activities. For these reasons glucosinolates are not uniformly distributed on the leaf, but are concentrated on the mid vein ⁽¹²⁾.

Humans frequent consumption of high glucosinolate content vegetables is associated with a lowered risk of cancer and cardiovascular disease. Interestingly, one of the most concentrated glucosinolate present in leaves of *Eruca Sativa* is glucoraphanin which is generated after hydrolysis sulphoraphane. This is recognized as the most effective compound which promotes the liver to produce enzymes that detoxify cancer-causing chemicals, especially those connected to chemically induced breast cancer and colon cancer ⁽¹³⁾. Anti-carcinogenic properties of glucosinolates and their associated hydrolytic products, isothiocyanates, have been shown in literature ^(14,15,16).

It has been shown that the major glucosinolate present in rocket leaves is 4-mercaptobutylglucosinolate (glucosativin), probably derived from S-demethylalkylation of 4-methylthiobutylglucosinolate (glucoerucin). This glucosinolate is associated to the characteristic pungent taste and flavor of this herb, that is different from other *Brassicaceae* ⁽¹⁷⁾. Other main glucosinolates have been identified in rocket plant, including 4-(β-D-glucopyranosyldisulfanyl) butyl glucosinolate ⁽¹⁸⁾, 4-methylthiobutyl glucosinolate (glucoerucin) mainly in seeds and roots ⁽¹⁹⁾, and 4-methylsulfinylbutyl glucosinolate (glucoraphanin) mainly in flowers ⁽²⁰⁾.

A complete report of the glucosinolates identified in rocket leaves (both species *Eruca stiva* and *Diplotaxis*) in literature and compared to the previous authors is shown in Table 1.3 ⁽⁹⁾.

The extraction has been done using methanol, and the identification of glucosinolates has been done by HPLC-DAD-ESI-MS. Eight desulfoglucosinolates has been identified from their protonated molecular ions $[M+H]^+$ and two main product ions, corresponding to the adducts $[M+Na]^+$ and $[M+K]^+$ compared to literature information.

Table 1.3 :Identification of desulphoglucosinolates of *Eruca* and *Diplotaxis*

#	Rt (min)	Mass data ESI ⁺	R-group ^a	Common name	References
A	7.1	380 $[M+Na]^+$, 396 $[M+K]^+$, 358 $[M+H]^+$ 196 $[aglycone+H]^+$	4-(Methylsulfinyl)butyl	Glucoraphanin	Bennett et al. (2002) D'Antuono et al. (2008)
B	8.5	394 $[M+Na]^+$, 410 $[M+K]^+$	5-(Methylsulfinyl)pentyl	Glucosalysin	D'Antuono et al. (2008) Kim et al. (2010)
C	8.9	410 $[M+Na]^+$, 426 $[M+K]^+$	2-(Benzoyloxy)ethyl 3-hydroxy-5-(methylsulfinyl)pentyl 5-(methylsulfonyl)pentyl	- - -	Fahey et al. (2001)
D	9.1	368 $[M+Na]^+$, 384 $[M+K]^+$	4-Hydroxybenzyl	Glucosinalbin	Kiddle et al. (2001) Bennett et al. (2007) D'Antuono et al. (2008)
E	10.4	544 $[M+Na]^+$, 560 $[M+K]^+$	4- $[\beta$ -D-Glucopyranosyl)disulfanyl) butyl)	4-GDB-GLS	Kim et al. (2004)
F	10.8	407 $[M+Na]^+$, 423 $[M+K]^+$	4-Hydroxy-3-indolylmethyl	4-Hydroxyglucobrassicin	Griffiths, Bain, Deighton, Botting, and Robertson (2000) Cataldi et al. (2007) Hong, Kim, and Kim (2011) Bennett et al. (2002)
G	11.5	350 $[M+Na]^+$, 366 $[M+K]^+$, 328 $[M+H]^+$ 166 $[aglycone+H]^+$	4-Mercaptobutyl	Glucosativin	Griffiths et al. (2000) Bennett et al. (2002) Kim et al. (2004)
H	13.4	364 $[M+Na]^+$, 380 $[M+K]^+$, 342 $[M+H]^+$ 180 $[aglycone+H]^+$	4-(Methylthio)butyl	Glucoerucin	Cataldi et al., 2007 D'Antuono et al. (2008) Kiddle et al. (2001) Cataldi et al. (2007) D'Antuono et al. (2008) Griffiths et al. (2000) Kim and Ishii (2006) Cataldi et al. (2007) Hong et al. (2011)
I	14.5	332 $[M+Na]^+$, 348 $[M+K]^+$	(R,S)-2-Hydroxy-3-butenyl	Progoitrin/epiprogoitrin	Bennett et al. (2002) Kim et al. (2004) Kim and Ishii (2006) Bennett et al. (2007)
L	14.8	391 $[M+Na]^+$, 407 $[M+K]^+$, 369 $[M+H]^+$	3-Indolylmethyl	Glucobrassicin	Bennett et al. (2002) Kim et al. (2004) Kim and Ishii (2006) Bennett et al. (2007)
M	16.7	675 $[M+Na]^+$, 691 $[M+K]^+$, 653 $[M+H]^+$ 490 $[aglycone+H]^+$, 529 $[aglycone+K]^+$ 513 $[aglycone+Na]^+$, 479 $[aglycone-S,+Na]^+$	Dimeric 4-mercaptobutyl	DMB-GLS	Bennett et al. (2002) Kim et al. (2004) Kim and Ishii (2006) Bennett et al. (2007)

^a The semi-systematic names of glucosinolates include the name of the R-group followed by the suffix-glucosinolate, e.g., 4-(methylsulfinyl)butyl glucosinolate for number 1.

The 8 glucosinolates identified can be classified as four aliphatic-derived (glucoraphanin, glucosalysin, glucoerucin and progoitrin/epiprogoitrin), one aromatic (glucosinalbin), two indole-derived compounds (4-OH-glucobrassicin and glucobrassicin) and two structurally related compounds containing one intermolecular disulfide linkage (4- $[\beta$ glucopyranosyl)disulfanyl) butyl glucosinolate and dimeric 4-mercaptobutylglucosinolate. The quantitative analysis results of glucosinolate content referred to the previous table is shown in the following Table 1.4 (°).

Table 1.4 : Total glucosinolate content of individuals compound in *Eruca* (SR) and *Diplotaxis* (WR)

Institute code	Accession code	Samples	A	B	C	D	E	F	H	I	L	M	TGC (mg kg ⁻¹ d.w.)
			%										
Sativa	6387300	SR1	23.4 ^{e-i}	0.5 ^{ab}	0.3 ^b	0.1 ^f	6.2 ^{b-x}	2.8 ^{b-d}	22.3 ^{b-i}	10.7 ^{b-i}	1.0 ^{e-x}	32.7 ^{a-c}	1707.3 ^{b-h}
DEU 146	ERU 12	SR4	53.8 ^{b-x}	0.4 ^{ab}	0.6 ^{ab}	0.1 ^f	3.6 ^x	3.0 ^{cd}	19.2 ^{h-p}	6.0 ^{lm}	1.4 ^{d-x}	12.0 ^c	1210.7 ^{e-i}
DEU 146	ERU 13	SR5	46.3 ^{b-t}	0.7 ^a	0.5 ^{ab}	0.1 ^f	4.2 ^{e-x}	3.3 ^{b-d}	22.0 ^{e-o}	4.9 ^{lm}	1.6 ^{b-t}	16.5 ^{b,c}	1424.9 ^{c-i}
DEU 146	ERU 14	SR6	22.4 ^{e-i}	0.3 ^{ab}	0.2 ^b	0.1 ^f	8.3 ^{a,b}	2.5 ^{a-d}	18.8 ^{b-n}	11.4 ^{b-f}	0.6 ^{e-x}	35.4 ^{a-c}	1958.8 ^{b-x}
DEU 146	ERU 15	SR7	23.8 ^{f-i}	0.4 ^{ab}	0.2 ^b	0.1 ^f	5.6 ^{b-x}	2.9 ^{cd}	25.0 ^{c-n}	6.5 ^{b-m}	1.2 ^{e-x}	34.2 ^{a-c}	1434.7 ^{c-i}
DEU 146	ERU 16	SR8	30.9 ^{f-i}	0.3 ^{ab}	0.2 ^b	0.1 ^f	5.9 ^{b-x}	1.7 ^{cd}	15.9 ^{x-o}	7.2 ^{e-m}	0.8 ^{e-x}	37.0 ^{a-c}	1837.0 ^{b-x}
DEU 146	ERU 17	SR9	29.1 ^{e-i}	0.3 ^{ab}	0.3 ^b	0.1 ^f	6.5 ^{b-x}	2.2 ^{cd}	17.1 ^{k-p}	9.6 ^{c-i}	1.0 ^{d-x}	33.8 ^{a-c}	1612.1 ^{b-i}
DEU 146	ERU 18	SR10	20.5 ^{e-i}	0.4 ^{ab}	0.2 ^b	0.1 ^f	6.7 ^{a-d}	3.5 ^{a-d}	24.0 ^{b-e}	11.1 ^{b-d}	0.9 ^{b-x}	32.7 ^{a-c}	2176.5 ^{a-d}
DEU 146	ERU 19	SR11	28.2 ^{d-i}	0.2 ^b	0.2 ^b	0.0 ^f	5.6 ^{b-x}	2.6 ^{cd}	22.5 ^{b-i}	6.6 ^{x-m}	1.0 ^{e-x}	33.0 ^{a-c}	1733.4 ^{b-h}
DEU 146	ERU 20	SR12	31.7 ^{c-i}	0.3 ^{ab}	0.1 ^b	0.0 ^f	5.3 ^{b-x}	2.0 ^{cd}	21.7 ^{b-m}	5.6 ^{i-m}	0.9 ^{d-x}	32.6 ^{a-c}	1731.3 ^{b-h}
DEU 146	ERU 21	SR13	24.9 ^{e-i}	0.3 ^{ab}	0.2 ^b	0.0 ^f	5.1 ^{b-x}	2.5 ^{b-d}	28.0 ^{b-d}	7.9 ^{d-m}	1.0 ^{e-x}	30.0 ^{a-c}	1882.6 ^{b-x}
DEU 146	ERU 22	SR14	22.8 ^{x-i}	0.3 ^b	0.1 ^b	0.0 ^f	4.7 ^{e-x}	5.4 ^{a-d}	24.7 ^{d-o}	5.5 ^{lm}	1.6 ^{b-x}	34.9 ^{a-c}	1319.1 ^{d-i}
DEU 146	ERU 23	SR15	39.6 ^{c-i}	0.4 ^{ab}	0.1 ^b	0.1 ^f	4.6 ^{e-x}	2.2 ^{cd}	16.7 ^{i-p}	5.0 ^{lm}	1.6 ^{b-x}	29.7 ^{a-c}	1319.3 ^{d-i}
DEU 146	ERU 24	SR16	28.4 ^f	0.4 ^b	0.3 ^b	0.1 ^f	6.0 ^x	5.4 ^{cd}	16.7 ^{o,p}	8.4 ^{lm}	1.7 ^{b-e}	32.5 ^{b,c}	756.0 ^f
DEU 146	ERU 26	SR17	22.1 ^{f-i}	0.2 ^b	0.1 ^b	0.0 ^f	4.1 ^{e-x}	3.1 ^{b-d}	24.1 ^{b-n}	4.3 ^{lm}	1.3 ^{b-x}	40.5 ^{a-c}	1507.5 ^{c-i}
DEU 146	ERU 27	SR18	41.1 ^{b-e}	0.4 ^{ab}	0.2 ^b	0.0 ^f	6.0 ^{b-x}	2.1 ^{cd}	19.8 ^{c-n}	6.8 ^{e-m}	1.3 ^{b-x}	22.4 ^{a-c}	1781.9 ^{b-h}
DEU 146	ERU 28	SR19	26.3 ^{h,i}	0.3 ^b	0.3 ^b	0.0 ^f	4.6 ^x	2.1 ^d	9.5 ^p	5.6 ^m	1.9 ^{d-x}	49.5 ^{a-c}	868.4 ^{h,j}
DEU 146	ERU 29	SR20	22.3 ^{d-i}	0.2 ^{ab}	0.2 ^b	0.0 ^f	6.1 ^{a-t}	2.1 ^{cd}	25.9 ^{b,c}	6.3 ^{e-m}	0.9 ^{f-x}	36.1 ^{a-c}	2139.6 ^{a-e}
DEU 146	ERU 30	SR21	21.1 ^{c-i}	0.2 ^{ab}	0.1 ^b	0.0 ^f	6.0 ^{a-c}	3.3 ^{a-c}	23.5 ^b	7.7 ^{b-i}	0.9 ^{b-x}	37.2 ^a	2459.0 ^{a,b}
DEU 146	ERU 33	SR22	35.1 ^{b-x}	0.2 ^b	0.1 ^b	0.0 ^f	6.5 ^{b-x}	2.7 ^{b-d}	18.2 ^{d-o}	10.9 ^{b-h}	0.5 ^{f-x}	25.7 ^{a-c}	1787.2 ^{b-h}
DEU 146	ERU 34	SR23	32.2 ^{c-h}	0.3 ^{ab}	0.1 ^b	0.1 ^f	5.5 ^{b-x}	3.0 ^{a-d}	28.1 ^{b-f}	7.3 ^{d-m}	0.9 ^{d-x}	22.5 ^{a-c}	1796.0 ^{b-h}
DEU 146	ERU 60	SR25	59.5 ^{b-d}	0.4 ^{ab}	0.1 ^b	0.0 ^f	3.6 ^{x,f}	2.7 ^{cd}	12.2 ^{m-p}	7.3 ^{b-m}	1.7 ^{b-e}	12.4 ^c	1393.3 ^{d-i}
DEU 146	ERU 94	SR26	59.6 ^b	0.3 ^{ab}	0.1 ^b	0.1 ^f	3.7 ^{e-x}	2.8 ^{cd}	12.0 ^{i-p}	7.5 ^{f-m}	1.2 ^{b-x}	12.7 ^{b,c}	1581.7 ^{b-i}
DEU 146	ERU 107	SR27	29.0 ^{f-i}	0.4 ^b	0.2 ^b	0.0 ^f	5.6 ^{c-x}	2.6 ^{cd}	15.4 ^{i-p}	11.3 ^{d-m}	1.4 ^{d-x}	34.2 ^{a-c}	1200.8 ^{e-i}
DEU 146	ERU 108	SR28	32.2 ^{f-i}	0.3 ^b	0.3 ^b	0.1 ^f	5.1 ^{e-x}	3.2 ^{cd}	15.0 ^{n-p}	7.7 ^{i-m}	0.8 ^{f-x}	35.3 ^{a-c}	1109.5 ^{x-i}
DEU 146	ERU 135	SR29	25.0 ^{e-i}	0.3 ^b	0.3 ^b	0.1 ^f	8.4 ^{a,t}	3.7 ^{a-d}	13.4 ^{i-p}	16.7 ^{a-c}	0.8 ^{e-x}	31.3 ^{a-c}	1524.9 ^{b-i}
DEU 146	ERU 140	SR30	37.6 ^{c-i}	0.4 ^{ab}	0.2 ^b	0.1 ^f	4.4 ^{d-x}	4.1 ^{a-d}	25.2 ^{b-n}	7.1 ^{k-m}	1.2 ^{e-x}	19.7 ^{a-c}	1467.2 ^{c-i}
DEU 146	ERU 143	SR31	27.0 ^{f-i}	0.4 ^{ab}	0.2 ^b	0.1 ^f	7.4 ^{a-z}	3.6 ^{a-d}	16.1 ^{f-o}	13.9 ^{ab}	0.8 ^{e-x}	30.6 ^{a-c}	1888.2 ^{b-x}
DEU 146	ERU 153	SR32	63.0 ^a	0.3 ^{ab}	0.2 ^b	0.1 ^f	3.0 ^{e-x}	1.8 ^{cd}	7.7 ^{n-p}	5.1 ^{k-m}	0.4 ^x	18.5 ^{a-c}	2083.7 ^{a-f}
DEU 146	ERU 154	SR33	34.3 ^{e-i}	0.3 ^b	0.2 ^b	0.1 ^f	5.2 ^{e-x}	2.3 ^{cd}	17.7 ^{i-p}	8.7 ^{h-m}	1.1 ^{b-x}	30.2 ^{a-c}	1159.9 ^{f-i}
DEU 146	ERU 158	SR34	36.8 ^{b,c}	0.3 ^{ab}	0.2 ^b	0.1 ^f	5.6 ^{a-t}	4.8 ^a	18.9 ^{b-h}	9.0 ^{b-x}	1.4 ^c	22.9 ^{a-c}	2352.3 ^{a-c}
Test ^A	242,152	SR37	20.2 ^{e-i}	0.2 ^{ab}	0.2 ^b	0.0 ^f	4.5 ^{b-x}	3.0 ^{a-d}	20.4 ^{b-i}	11.5 ^{b-e}	10.4 ^a	29.4 ^{a-c}	1965.0 ^{b-x}
Sativa	PISTIC4367500	WR2	36.1 ^{e-i}	0.2 ^b	1.1 ^a	1.7 ^b	5.5 ^{c-x}	2.1 ^d	23.8 ^{x-o}	6.0 ^{lm}	1.9 ^{b-f}	21.6 ^{a-c}	1220.3 ^{e-i}
Sativa	PISTIC4369500	WR3	17.6 ^f	0.3 ^b	0.3 ^b	0.7 ^d	7.4 ^{b-x}	3.5 ^{cd}	18.9 ^{i-p}	12.3 ^{d-m}	2.1 ^{b-e}	36.7 ^{a-c}	1164.2 ^{f-i}
ITA004	RIU47	WR24	20.6 ^{b-x}	0.2 ^{ab}	0.0 ^b	0.9 ^a	6.9 ^a	3.4 ^{a,b}	27.3 ^a	11.5 ^a	1.1 ^{b-d}	28.1 ^{ab}	3031.1 ^a
Test ^A	241,803	WR35	27.7 ^{e-i}	0.4 ^{ab}	0.1 ^b	0.6 ^c	4.4 ^{c-x}	4.9 ^{a-c}	26.3 ^{b-x}	6.5 ^{k-m}	2.0 ^p	27.0 ^{a-c}	1709.7 ^{b-h}
Test ^A	242,870	WR36	27.6 ^{e-i}	0.4 ^{ab}	0.2 ^b	0.4 ^e	6.2 ^{b-x}	3.7 ^{a-d}	22.9 ^{d-o}	11.5 ^{b-i}	1.2 ^{e-x}	25.9 ^{a-c}	1465.5 ^{c-i}

A, glucoraphanin; B, glucoalyssin; C, 2-(benzoyloxy)ethyl/3-hydroxy-5-(methylsulfonyl)pentyl/5-(methylsulfonyl)pentyl; D, glucosinalbin; E, 4-GDB-GSL; F, 4-hydroxyglucobrassicin; H, glucoerucin; I, progointrin/epiprogoitrin; L, glucobrassicin; M, DMB-GLS; TGC, total glucosinolate content.

^A Controls from Warwick University (UK).

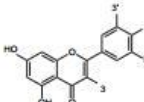
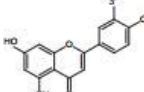
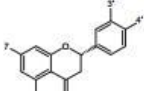
The total average glucosinolate content is 1642.2 mg/kg D.W., and ranged from 756.0 to 2459.0 mg/kg D.W. and from 1164.2 to 3031.1 mg/kg D.W. for *Eruca* and *Diplotaxis* respectively. DMB-GLS is taken in consideration for the total and relative GLS quantification. The aliphatic glucosinolates are predominant representing over 60% of total glucosinolates. The main components are glucoarephanin, DMB-GLS and glucoerucin. Glucoaraphanin (A) ranged from 17.6% to 63 %, has the highest relative percentage. DMB-GLS (M) together with (4GDB-GLS) ranged from relative percentage 12% to 49.5 %. Glucoerucin (H) relative content ranged from 7.7 % to 28.1 %. Indole (4-OH-glucoerucin, F, and glucobrassicin, L) and aromatic (glucosinalbin, D) represent a lower part of total glucosinolate composition.

1.2.2 Polyphenols

Tissues of rocket salad contain significant concentrations of flavonoids. Flavonoids are a class of plant secondary metabolites, that are mostly distributed in fruits, vegetables and the leaves

of herbal plants. Moreover, they are the most important plant pigments for flower coloration (their name derives from the Latin word “flavus” meaning yellow, their colour in nature). Flavonoids are polyphenolic compounds that are often added to medicines as antioxidants. They can significantly reduce damage associated with conditions such as cancer and cardiovascular disease ⁽²¹⁾. For example, flavonoids are poorly absorbed in the proximal gastrointestinal tract and are therefore likely to reach the colon in substantial quantities, protecting the colonic epithelium from free radical attack ⁽²²⁾. Their nuclear structure comprise two benzene rings connected by a pyrene ring containing oxygen. Usually, they are classified into sub groups including flavonols, flavones, flavanols, flavanones, and isoflavones based on the additional presence of a C2-C3 double bond, hydroxyl, methoxy groups, glycoside, and different positions of molecules. A classification is shown in Table 1.5 ⁽²³⁾.

Table 1.5 : Classification of flavonoids from plants according to their skeletal formula.

Flavonoid group	Compound	Skeletal formula	3'	4'	3	7	Plant sources
Flavonol	Quercetin		OH	OH	OH	-	Onion skin
	Isorhamnetin		O-CH ₃	OH	OH	-	Sea-buckthorn leaves
	Kaempferol		H	OH	OH	-	Carrot
	Spiraeoside		OH	O-glucose	OH	-	Onion skin
	Quercitrin		OH	OH	O-rhamnose	-	Saururus chinensis
	Isoquercitrin		OH	OH	O-glucose	-	Saururus chinensis
Flavone	Apigenin		H	-	-	-	Parsley
	Luteolin		OH	-	-	-	Carrot
Flavanone	Naringenin		H	OH	-	OH	Grapefruit
	Hesperetin		OH	O-CH ₃	-	OH	Lemon
	Narirutin		H	OH	-	O-rutinoside	Grapefruit
	Naringin		H	OH	-	O-neohesperidose	Grapefruit
	Hesperidin		OH	O-CH ₃	-	O-rutinoside	Orange

The identification of the polyphenolic compounds in the rocket salad was found in literature ⁽⁹⁾. It was based on chromatographic behavior, mass spectra obtained under electron spray ionization (ESI) conditions and comparison with literature. The results are shown in table 1.6 for both the species of rocket salad, *Eruca* and *Diplotaxis*.

Table 1.6: Identification of phenolic compounds in *Diplotaxis* and *Eruca* samples

#	Rt (min)	Compound
<i>Diplotaxis</i> samples		
1	17.6	Quercetin-3,3',4'-triglucoside
2	22.0	Quercetin-3,4'-di-glucoside-3'-(6-methoxycaffeoyl-glucoside)
3	22.8	Quercetin-3,4'-di-glucoside-3'-(6-caffeoylglucoside)
4	24.2	Isorhamnetin-3,4 diglucoside
5	25.5	Quercetin-3,4'-di-glucoside-3'-(6-sinapoyl-glucoside)
6	26.7	Quercetin-3,4'-di-glucoside-3'-(6-feruloyl-glucoside)
7	27.7	Quercetin-3,4'-di-glucoside-3'-(6-p-coumaroyl-glucoside)
8	30.3	Quercetin-3-(2-sinapoyl-glucoside)-3'-(6-sinapoyl-glucoside)-4'-glucoside
9	31.0	Quercetin-3-(2-feruloyl-glucoside)-3'-(6-sinapoyl-glucoside)-4'-glucoside
10	32.7	Quercetin-3-(2-feruloyl-glucoside)-3'-(6-feruloyl-glucoside)-4'-glucoside
<i>Eruca</i> samples		
11	17.8	Kaempferol-3-diglucoside-7-glucoside
12	21.4	Kaempferol-3-sinapoyl-triglucoside-7-glucoside
13	22.8	Kaempferol-3,4-diglucoside
4	24.2	Isorhamnetin-3,4 diglucoside
14	29.6	Quercetin-3-glucoside
15	33.7	Kaempferol-3-glucoside
16	33.9	Isorhamnetin-3-glucoside
17	35.0	Kaempferol-3-(2-sinapoyl-glucoside)-4'-glucoside

As can be seen in Table 1.6, Quercetin and Kaempferol derivatives are the major group of phenolic compounds in these species. The investigation on flavonoid content shows that *Diplotaxis* are characterized by quercetin derivatives as the main component. The average total flavonoids content is 12.35 g/kg D.W., ranged from 4.68 to 19.81 g/kg D.W., while *Eruca* samples shows a variability of total flavonoid content. The average total flavonoid content of *Eruca* is 25.53 g/kg D.W., ranged from 9.99 to 31.39 g/kg D.W. The most abundant flavonoid are kaempferol derivatives ranging from 8.47 to 26.0 g/kg D.W. (77-88 of total phenolics). Kaempferol-3,4-diglucoside (ranging 8.07 to 23.68 g/kg) and Isohamnetin-3,4-diglucoside are respectively the first and the second flavonoid present.

1.2.3 Fatty Acids

Fatty acids are carboxylic acids with a long aliphatic chain. Usually the number of carbon atoms in the chain is between 4 and 28. Depending on the length of the aliphatic chain fatty acids are classified as short-chain (up to 6 carbon atoms), medium chain (from 6-12), long chain (13-21) and very long chain (more than 22). The chain can be saturated or unsaturated if there are one or more carbon-carbon double bond. The two carbon atoms in the chain that are bound next to either side of the double bond can occur in a "cis" or "trans" configuration, see Figure 1.8.

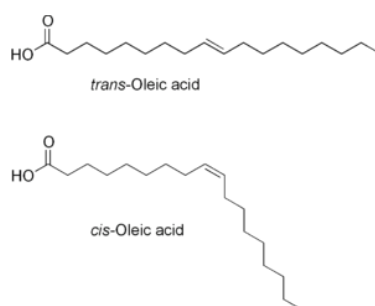


Figure 1.8 : Comparison between trans and cis isomer of oleic acid

A “cis” configuration means that the hydrogen atoms are on the same side of the double bond, while a trans configuration means that the next hydrogen atoms are on the opposite sides of the double bond. Naturally sources of fatty acids are rich in “cis” isomer.

The differences in geometry between the various types of unsaturated fatty acids, as well as between saturated and unsaturated fatty acids, play an important role in biological processes. A fatty acid chain is monounsaturated if it contains one double bond, and polyunsaturated if it contains more than one double bond. There are called essential fatty acids, since human must ingest because the body is not able to synthesize them (only two acids are essentials alpha-linoleic acid and linoleic acid). In cellular metabolism, unsaturated fatty acids contain less energy than the correspondent saturated acid (which has already the maximum of hydrogen atoms bond). The greater the degree of unsaturation in a fatty acid (number of double bonds), the less energy is required for its degradation.

The study of importance on unsaturated fatty acids for human health has gained more and more importance in recent years. Unsaturated fats helps to lower levels of total cholesterol and LDL (low density lipoprotein) in the blood, and are known to prevent cardiovascular disease. Examples of unsaturated fats are palmitoleic acid, oleic acid, myristoleic acid, linoleic acid, and arachidonic acid. Foods containing unsaturated fats include avocado, nuts, and vegetable oils such as canola and olive oils.

In literature, the identification of fatty acids in rocket leaves has not been reported. However, the composition of the seed-oils of rocket is available. The oil content and the fatty acids composition of the *Eruca sativa* seeds is shown in Table 1.7 (6).

Table 1.7 : Fatty acids content and composition of *Eruca Sativa* lines

Line no.	Origin	Oil content %	Fatty acid (% of total)						
			Palmitic C 16:0	Stearic C 18:0	Oleic C 18:1	Linoleic C 18:2	Linolenic C 18:3	Eicosenoic C 20:1	Erucic C 22:1
1/96	Germany	29.1 a	*5.1 a**	1.3 b	15.1 a	8.3 b	14.7 b	7.4 b	44.7 a
2/96	Italy	28.7 a	4.9 a	1.4 b	16.7 a	10.3 b	14.6 b	7.3 b	42.8 a
6/96	Italy	27.8 ab	4.8 a	1.6 b	15.2 a	9.4 b	15.2 b	7.6 b	43.3 a
16/95	Italy	28.8 a	4.8 a	1.4 b	15.9 a	9.5 b	15.1 b	7.6 b	43.3 a
14/96	Israel-Matt.	27.8 ab	4.7 a	1.4 b	17.8 a	9.4 b	14.9 b	7.5 b	42.4 a
18/96	Israel-Matt.	27.8 ab	5.2 a	1.4 b	16.9 a	9.6 b	14.9 b	7.4 b	41.7 a
3/96	Israel-Yair	24.8 c	4.1 b	1.5 b	9.9 b	14.1 a	19.7 a	9.8 a	37.0 b
20/96	Israel-Yair	26.2 b	4.0 b	1.9 a	11.4 b	14.0 a	18.8 a	9.4 a	36.3 b
21/96	Israel-Yair	25.6 bc	4.2 b	1.8 a	11.5 b	14.8 a	19.2 a	9.6 a	35.2 b
22/96	Israel-Yair	25.5 bc	4.0 b	1.9 a	12.6 b	15.3 a	18.9 a	9.4 a	33.4 b

* Numbers are averages of four replications.

** Different letters indicate significant differences for each parameter separately at $P < 0.05$ (Duncan's Multiple Range Test).

Oil content varies from 24.5 to 29.2 %, depending on the origin of the herb. *Eruca sativa* as a member of *Brassicaceae* contains erucic acid (C22:1), a fatty acid unique to seed oils which varies from 33 to 47 %. For Italian origin rocket salad, its concentration is average 43 %.

Linolenic (C18:3) and oleic (C18:1) are also present with an average content of 15.9 and 15.1%. Eicosenic stearic and palmitic are present in lower quantity.

The ratio of mono-unsaturated fatty acids (oleic, C18:1; eicosenoic C20:1 and erucic, C22:1) to polyunsaturated fatty acids (linoleic, C18:2; and linolenic, C18:3) is shown in Table 1.8 .

Table 1.8 : Ratio of monounsaturated/polyunsaturated fatty acids in *Eruca sativa* lines

Line no.	Origin	Fatty acid (% of total)	
		C 18:1 + C 20:1 + C 22:1	C 18:2 + C 18:3
1/96	Germany	67.2	23.0
2/96	Italy	66.8	24.9
6/96	Italy	66.1	24.6
16/95	Italy	66.8	24.6
14/96	Israel-Matt.	67.7	24.3
18/96	Israel-Matt.	66.0	24.5
3/96	Israel-Yair	56.7	33.8
20/96	Israel-Yair	57.1	32.8
21/96	Israel-Yair	56.3	34.0
22/96	Israel-Yair	55.4	34.2

1.3 Literature review on supercritical CO₂ extraction of glucosinolates, flavonoids and fatty acids from rocket salad

Since literature is not particularly furnished with works on the supercritical CO₂ extraction of the compounds from rocket salad, a review on the supercritical extraction of the same compounds from other vegetables is reported. Methods and results of these works are briefly shown below.

1.3.1 Supercritical CO₂ extraction of glucosinolates

Glucosinolates have been extracted with supercritical CO₂ from canola meal (²⁴). Canola is the major oilseed crop grown in Canada. It belongs to the same family of rocket salad (*Brassicaceae*). Canola is mainly utilized because of its oil, the residual meal is a valuable source of protein and it is used as animal feed (²⁴). Since glucosinolates are toxic for herbivores they have to be removed from the meal.

The supercritical CO₂ extraction has been performed at 70°C and 40 MPa for 6 hours. The extraction cell has been loaded with 10 g of meal. The flow rate of CO₂ have been maintained at 1 L/min and added continuously with ethanol (20 % w/w). The glucosinolate contents of the canola meals extracted with SCCO₂ was 5.6-6.8 µmol/g, while glucosinolates available was 6.9-7.96 µmol/g.

1.3.2 Supercritical CO₂ extraction of phenolic compounds (flavonoids)

Since flavonoids are widely distributed in fruits, vegetables and plants, and being their healthy properties well known, their extraction with supercritical CO₂ has been performed by several authors at various experimental conditions.

For example, supercritical CO₂ extraction of flavonoids has been performed on leaves of *Strobilanthes crispus* ⁽²⁵⁾. This is a vegetable herb commonly consumed in a form of herbal tea, proven to possess antioxidant activity and anticancer properties ^(26,27), for whom was identified the optimum processing variables for the supercritical CO₂ extraction. The optimum values of pressure, temperature and extraction time were respectively 200 bar, 50°C, and 60 min. The initial plant material was 30 grams and the flow rate of CO₂ and co-solvent (ethanol) were maintained at 10 and 1 g/min, respectively. The optimum yield (mass of extract / mass of feed) was 5.17 % with a flavonoids content of 3.98 % (mg of flavonoids / mg of extract). Supercritical CO₂ extraction of flavonoids has also been performed on leaves of *Ginkgo biloba*. In literature ⁽²⁸⁾ 90 grams of dry *Ginkgo* powder were extracted at 60°C and 31.2 MPa. The solvent was a mixture of SC-CO₂ and ethanol (10 mol %). The final yield was 8 % (mass of extract / mass of feed) with a flavonoids content of 183 µg / g.

1.3.3 Supercritical CO₂ extraction of lipids

In literature supercritical fluid extraction of lipids from leaves of rocket salad is not reported. However, supercritical fluid extraction has been performed to extract lipids from leaves of broccoli (*Brassica oleracea L. var. Italica*). This is a vegetable that belongs to the family of *Brassicaceae*, that includes also rocket salad. Supercritical fluid extraction of lipids from broccoli leaves has been performed in literature ⁽²⁹⁾. Lipids were extracted using pure CO₂ obtaining the best results at 60° C, 300 bar, 3mL/ min and an extraction time of 90 min. Since at these conditions the more polar fraction of lipids remain in the residual material, another extraction has been performed employing a co-solvent. Methanol was used as co-solvent obtaining the maximum of yield with 15 % methanol. Twenty-three fatty acids were identified in the extracts. Among them, α -linoleic, linoleic and palmitic acids were the most abundant ⁽²⁹⁾.

CHAPTER 2

MATERIALS AND METHODS

Raw material samples have been freeze-dried before extraction tests, to reduce the water content. Supercritical carbon dioxide extraction has been done using a supercritical extraction laboratory plant. An extraction with a Soxhlet apparatus has been performed too. The extracts have been analysed using HPLC-MS and NMR.

2.1 Pre-treatment: Lyophilization of the leaves

Leaves of rocket salad have been bought in a local market. Water content in the raw leaves has been reported to be around 91 wt. % (³⁰). Water can interfere with extraction, hence a pre-treatment is required to dry the leaves. Usually drying methods use high temperatures that can damage the internal structure of biological compounds. In order to keep the internal structure of the leaves intact, lyophilization seems to be the most appropriate technique.

This process, also known as freeze-drying is a dehydration method that works by freezing the material and then reducing the pressure to allow to the frozen water in the material to sublime directly from the solid phase to the gas phase. Freeze-drying does not usually cause shrinkage or toughening of the material being dried. In addition, flavours, smells and nutritional content generally remain unchanged, making the process popular for preserving food. However, water is not the only chemical capable of sublimation, and can be losses of other volatile compounds such as acetic acid and alcohols can occur.

Freeze-drying is mostly used in pharmaceutical and food industry to increase the shelf life of the products. Preservation is possible because the greatly reduced water content inhibits the action of microorganisms and enzymes that would normally spoil or degrade the substance. Moreover, foods which are lyophilized can usually be stored without refrigeration, which results in a significant reduction of storage and transportation costs. Another advantage of using this technique of dehydration is that freeze-dried products can be rehydrated much more quickly and easily because the process leaves microscopic pores. The pores are created by the ice crystals that sublime, leaving gaps or pores in their place. Lyophilisation does not significantly reduce volume, therefore water quickly regains its place in the molecular structure of the food or product.

The stages of dry freezing are shown in the diagram of state reported in Figure 2.1 ⁽³¹⁾.

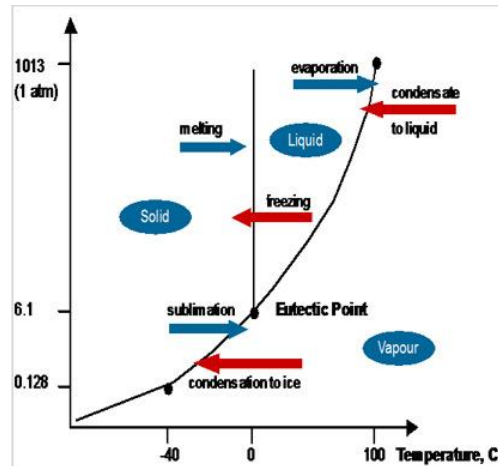


Figure 2.1: Water P-T phase diagram

Generally, the first stage is a pre-treatment of the product before freezing. This may include concentrating the product, formulation revision (i.e., addition of components to increase stability and/or improve processing), decreasing a high vapour pressure solvent or increasing the surface area. In our case, the raw leaves of rocket salad were milled to increase the surface area.

The second stage is freezing. The sample was placed in a freeze-drying flask and rotated in a bath, called shell freezer, cooled by liquid nitrogen. To allow the sublimation to occur rather than melting, in this step is important to go below the triple point. This stage is the most critical of the freeze-drying process. The freezing temperature is about $-50\text{ }^{\circ}\text{C}$.

The third stage is primary drying. During this step the pressure is lowered to a few millibar and enough heat to allow water to sublime is supplied to the sample. The heat is brought by conduction or radiation. About 95% of the water is sublimated. This step is very slow and can require several days. Increasing the heat supplied to lower the time could lead to the degradation of the biological material. In this stage pressure is controlled through the application of partial vacuum. Moreover, a cold condenser chamber and condenser plates provide a surface for the water vapour to solidify on. Condenser temperatures are below $-50\text{ }^{\circ}\text{C}$.

The secondary drying is usually added as a further stage. In this step the unfrozen water molecules are removed, the temperature is raised higher than in the primary drying phase, and can even be above $0\text{ }^{\circ}\text{C}$, to break any physico-chemical interactions that have formed between the water molecules and the frozen material. Usually the pressure is also lowered in this stage to encourage desorption (typically in the range of microbars, or fractions of a pascal).

An image of an apparatus for dry-freezing process is shown in Figure 2.2.



Figure 2.2: Freeze-drying equipment

Two components are common to all types of freeze-dryers: a vacuum pump to reduce the ambient gas pressure in a vessel, containing the substance to be dried, and a condenser to remove the moisture by condensation on a surface cooled until -40 to -80 °C.

After the dry-freezing process is completed the water content in our samples of rocket salad was about 4%, as was measured by gravimetric analysis.

A mechanical pre-treatment was also done. Dried leaves were grinded using a ceramic pestle to reduce their particles dimension (Figure 2.3).



Figure 2.3: Pestle

After that, particles were filtered with a metallic sieve characterized by dimension of pores of 0.5 mm.

2.2 Supercritical CO₂ extraction process

The experimental extraction work has been carried in the High-Pressure Laboratory of Industrial Engineering Department. The materials that have been used include:

- Leaves of rocket salad after pre-treatments (lyophilisation and mechanical milling)
- Carbon dioxide (99.998 %, gas cylinder of 50 L and 40 kg of carbon dioxide, Rivoira)
- Ethanol (99.5 %, Sigma Aldrich)
- Methanol (99.8 % Sigma Aldrich)
- Ultrapure water (Milli-Q, filtered by a 0.22 μm membrane)

The process is operated in a batch mode. The extraction cell is charged with the solid sample to be extracted. Then supercritical fluid added with co-solvent flows through the fixed bed and extracts the soluble molecules. The extract is then separated from the supercritical solvent by depressurization. The scheme of the laboratory extraction plant is shown in Figure 2.4 :

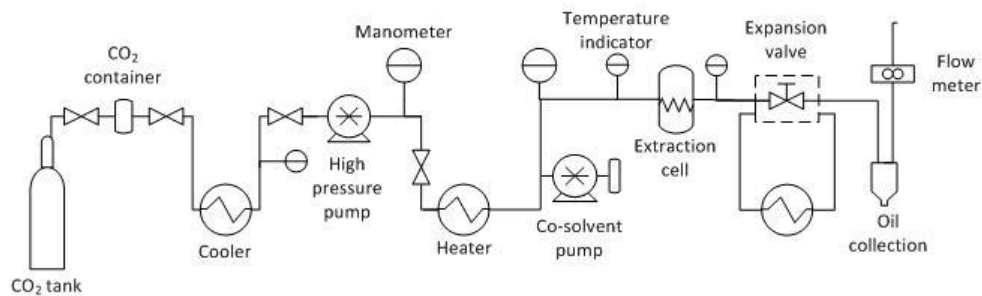


Figure 2.4 : Laboratory extraction plant

Carbon dioxide is contained in the tank cylinder. Another CO₂ container is used as a surge tank before the extraction process. During the experiments this is kept at constant pressure of about 60 bar. Carbon dioxide is then cooled down to liquid phase by a cooler in order to avoid the cavitation of the pump. The refrigerant used in the cooler is ethylene glycol. In the next step, carbon dioxide is sent to a high pressure pump to reach supercritical state. The pressure ranged from 150 to 300 bar. Manometers are used to indicate the pressure of the surge tank and before the extraction process. The supercritical solvent is heated up in a pre-heater before going to the extraction cell to reach the required temperature. The heat is supplied with an electric heating resistance around it. The temperatures ranged from 45 to 75 °C. The co-solvent is charged in a container of 500 ml and is sent to a pump to reach the same pressure of the supercritical fluid. The two solvents mix together and flow across the fixed bed of rocket salad charged in the extraction cell. Temperature indicators are placed before and after the extraction cell.

The extraction cell is a carbon steel cylinder made up of two screwed parts (Figure 2.5). The cylinder has a diameter of 5 cm and is long 11.5 cm. The thickness of the walls is 1 cm.



Figure 2.5: Extraction Cell

The right side of the Figure 2.5 shows the upper part with the inlet, while the left part shows the lower part with the outlet. The part on the right side is screwed with the left part leaving the emptiness of the solid chamber. The solvent flows through the hollow tube of small diameter (0.5 cm) from the upper part to the lower part.

The solid chamber is made up of the not threaded part, which includes the inner cylinder of 1.5 cm of diameter and the bigger cylinder of 3 cm of diameter. The solid is charged in the inner cylinder which is 1.5 cm long with a diameter of 1.5 cm, while the other cylinder is filled with a Teflon ring. A rubber o-ring gasket is wrapped around the tip of the upper part to avoid pressure losses.

The mass of solid charged in our tests was 0.49 ± 0.05 g. In order to avoid particle losses during the extraction a filter is put before the outlet. The filter is made up of two layers: an acetate membrane with pores of $0.22 \mu\text{m}$ to avoid losing particles and a metal mesh of diameter of 0.5 mm as support of the membrane at high pressures. The filled and assembled extraction cell is easily secured in the plant with two bolts and nuts (nominal hole diameter D of 9/16). The extraction cell is also insulated with a layer of fiberglass collected by an aluminum sheet to avoid thermal losses.

The temperature of the extraction cell is controlled by an electric resistance wrapped around the cell and connected to a temperature controller. Another temperature indicator is placed downstream of the extraction cell.

After the extraction cell, the loaded supercritical solvent added with co-solvent passes through the expansion valve. Hence the pressure is reduced to 1 atmosphere. Since the fluid is below the inversion temperature of carbon dioxide, the Joule-Thomson coefficient is positive, that means that the gas cools down when expands. The valve can be frozen, hence a heater is

required. For this purpose, the valve was immersed in a bath with recirculating warm water at about 45 °C.

The separation process takes place after the throttling valve, where carbon dioxide passes to gas phase and it is completely removed from the extract. The extract with the co-solvent is recovered and collected in a plastic flask. A small amount of solvent was placed in the plastic flask to recover the extract. Carbon dioxide goes to a volumetric flow rate meter and then to a displacement volumetric meter. Carbon dioxide flow rate is controlled with the opening degree of the valve. In the following Figure 2.6 a view of the plant is shown.



Figure 2.6 :View of the laboratory extraction plant

In the experimental tests the yield of the extraction was calculated as:

$$Yield = \frac{\text{Mass of oil extracted}}{\text{Mass of initial solid}} \quad (2.1)$$

Tests have been carried out at different experimental conditions in order to find out the highest yield of the extraction.

The extraction experimental procedure is:

1. 0.5 g of solid sample are weighted.
2. The filter is put in the extraction cell.
3. The extraction cell is charged with the solid and the Teflon ring and then assembled.
4. The cooler is switched on.
5. The thermostatic bath of the valve is turned on.
6. The extraction cell is secured in the plant with two bolts and nuts.

7. After the cooler temperature is enough to liquefy the CO₂ (5 °C), the valve of the CO₂ cylinder can be opened and CO₂ can flow to the pump.
8. A mixture of soap and water is sprinkled on the extraction cell for the leak test.
9. The valve upstream the extraction cell is opened and CO₂ is allow to flow in the extraction cell.
10. The set point of the CO₂ pump is fixed and the pump is switched on.
11. If leakages are present the mixture of soap and water will swell an bubbles will be seen. Then the pump have to be switched off, the valve upstream the extraction cell has to be closed, while the valve downstream the extraction cell has to be opened to depressurize the cell. The extraction cell has to be better secured to the plant (a layer of Teflon wrapped on the bolts and nuts can be a good solution). The procedure has to be repeated from number 7.
12. If there are not leakages the extraction cell can be pressurized until the desired pressure. Supercritical carbon dioxide permeates the solid in the cell and solubilize the low weight apolar components. The pump is then switched off, the valve upstream is closed and the valve downstream is opened to allow the depressurization of the extraction cell. The solubilized components are recovered in the separator. This is also a pre-treatment for the following extraction, hence supercritical CO₂ is permeated in the solid after depressurization and subsequently expansion the cells are broken and the following solvent can more easily access and solubilize the desired components.
13. The valve downstream the extraction cell is closed and that upstream is opened.
14. Temperature controllers are turned on.
15. The pump is turned on.
16. The extraction cell is pressurized so the downstream valve can be opened.
17. When the desired conditions of pressure and temperature are reached the co-solvent pump is turned on the same pressure of the supercritical CO₂: hence the two solvents can mix and flow to the extraction cell.
18. The chronometer is started : Beginning of the experimental test.
19. Each 10 minutes the collected extract is recovered in a test tube, and the carbon dioxide consumed is registered as reported in the displacement volumetric meter.
20. After 1 hour of extraction, 6 test tubes are collected.
21. The chronometer is stopped : End of the experiment test.
22. Both the pumps are switched off and the valve upstream the extraction cell is closed.
23. Temperature controllers are switched off.
24. The cooler is switched off and the valve of the cylinder tank is closed.
25. The valve downstream the extraction cell is fully opened to allow a complete depressurization.

26. After being cooled at environmental conditions, the extraction cell can be removed from the plant, cleaned, and ready for a new extraction.

After the extraction has been performed, there are 6 test tubes containing the oil extracted plus the co-solvent added. Figure 2.7 shows the samples collected during an experiment carried out in our laboratory.

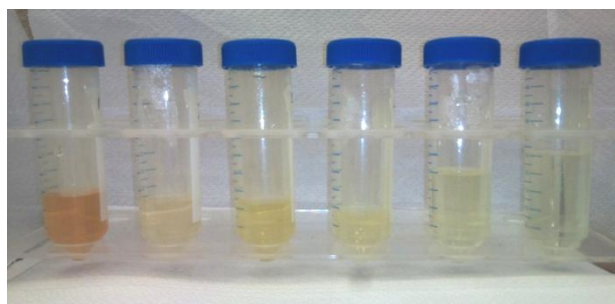


Figure 2.7: Extracted samples

Then a separation process is required. To achieve this target, a rotary evaporator is used (Figure 2.8)

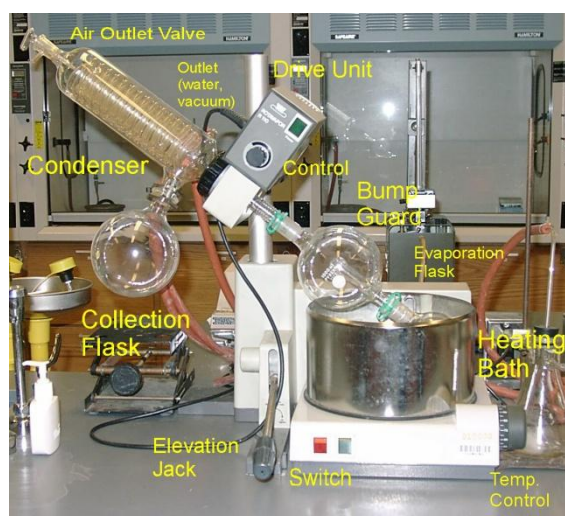


Figure 2.8 : Rotary evaporator

This device is mainly made up of a heating bath and a condenser. The extract added with the solvent to be separated is put in a flask. This is immersed in a heating bath that has to heat up enough to allow the solvent in the sample to evaporate. The sample is rotated by a drive unit in order to allow a uniform distribution of the heat in the sample. A vacuum pump is connected to allow evaporation at lower temperatures. After being evaporated, the solvent flows in the condenser, where cold water flows continuously. The vapor is then condensed

and completely recovered in the collection flask. Therefore only the extract remains in the evaporation flask, attached to the walls of the flask.

The temperatures set in the heating bath depend on the boiling temperature of the solvent to be separate and also on the temperature tolerated by the substance extracted before its degradation. Usually, to separate ethanol and methanol 48 °C has been set. To separate water, a temperature of 70 °C has been used.

To calculate the amount of extract this procedure is followed :

1. The empty flask (or matrass) is weighted.
2. The first sample is poured in the empty flask.
3. The flask is put in the rotary evaporator until the solvent is completely evaporated and the extract is precipitated.
4. The flask is weighted. The amount of the extract is calculated as the difference between this weight and the previous one.
5. The second sample is poured in the same flask.
6. The flask is put in the rotary evaporator until the solvent is completely evaporated and the extract is precipitated.
7. The flask is weighted.
8. The same steps from 5 to 7 are repeated until the last sample is done.

The difference between the final weight and the empty flask represents the total amount of oil extracted.

The experimental values of the yield vs mass of cumulated CO₂ are plotted. An empirical model is used to fit the data. The equation of the model is :

$$Y = \frac{K_1 * X}{K_2 + X} \quad (2.2)$$

Where Y = mass of oil extracted / mass of initial solid, X = mass of CO₂ / mass of initial solid and K_1 , K_2 re adjustable parameters.

The cumulated mass of CO₂ used during the experiment is calculated multiplying the volumetric value from the displacement volumetric meter per the density of carbon dioxide (1.98 kg/m³) at each experimental step and make the cumulative.

2.3 Soxhlet extraction

To compare the results obtained with the supercritical fluid extraction with a classical solvent extraction, a Soxhlet extraction has also been performed.

A typical apparatus is shown in the following Figure 2.10.

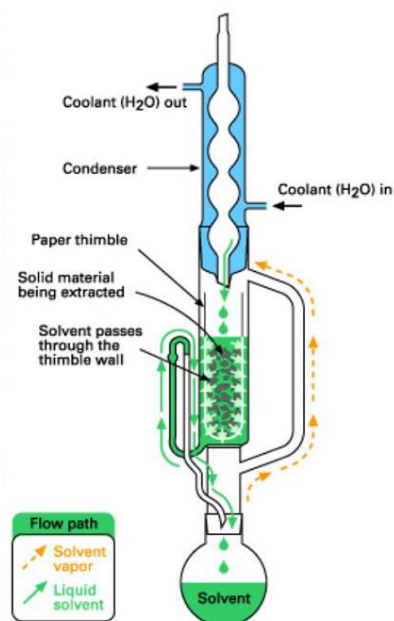


Figure 2.10 : Soxhlet extraction apparatus.

The apparatus is made up of three parts: a round bottom flask, the “soxhlet” extractor, and a condenser. The solvent is placed in the round bottom flask and is heated to allow its complete evaporation. A mixture of methanol and water 70:30 v/v has been used as solvent, heated at 100°C. The vaporized solvent flows to the condenser (the yellow path in figure 2.10), where coolant water flows continuously. The solvent condenses and falls to the “soxhlet” extractor. Here the solid to extract is placed in a paper thimble. The solvent is extracted from the solid and passes through the thimble wall (the green path in Figure 2.10). The extract is finally collected in the round bottom flask. The Soxhlet extraction was carried out for 20 hours.

2.4 Analysis of the extract

The extracted samples were analyzed in a laboratory of the Department of Pharmaceutical and Pharmacological Science. The identification and the content of glucosinolates, flavonoids and fatty acids were measured employing two techniques: HPLC-MS and NMR.

2.4.1 HPLC – MS

Liquid chromatography–mass spectrometry (LC-MS, or high performances liquid chromatography HPLC-MS, is an analytical chemistry technique that combines the physical separation abilities of liquid chromatography with the mass analysis capabilities of mass spectrometry (MS). It is generally used to separate, generally detect or to identify chemicals

of particular masses in presence of other chemicals. Principally, it is used to identify a natural product from a natural product extract or a pure substance from a mixture of other intermediates.

HPLC is a liquid chromatography separation technique that operates at relatively high pressures. As in liquid chromatography there is a mobile phase and a stationary phase. The sample is forced by a liquid at high pressures (mobile phase) through a column that is packed with a stationary phase composed by irregularly or spherically shaped particles depending on the separation target to achieve. Depending on the stationary phase and on the polarity of the mobile phase two methods of HPLC can be used. For reversed phase liquid chromatography (RP-LC) octadecylsilyl (C18) is used as stationary phase with organic-water mixture as mobile phase (water-acetonitrile and water-methanol). For normal phase liquid chromatography (NP-LC) silica gel is used as stationary phase with organic mixtures. Usually, the former is used as the means to introduce samples into the mass spectrometry. The flow used in the standard column (4.6 mm bore diameter) has to be split before sent to the column (10:1). The mass spectrometry will give improved sensitivity at flow rates of 200 $\mu\text{L}/\text{min}$ or less.

Mass spectrometry is an analytical technique that measures the mass to charge ratio of charged particles. MS works by ionizing chemical compounds to generate charged molecules or molecule fragments and measuring their mass-to-charge ratios. It is used for determining masses of particles for elucidating the composition of a sample or the structure of a molecule . A typical HPLC-MS coupling is shown in Figure 2.11.

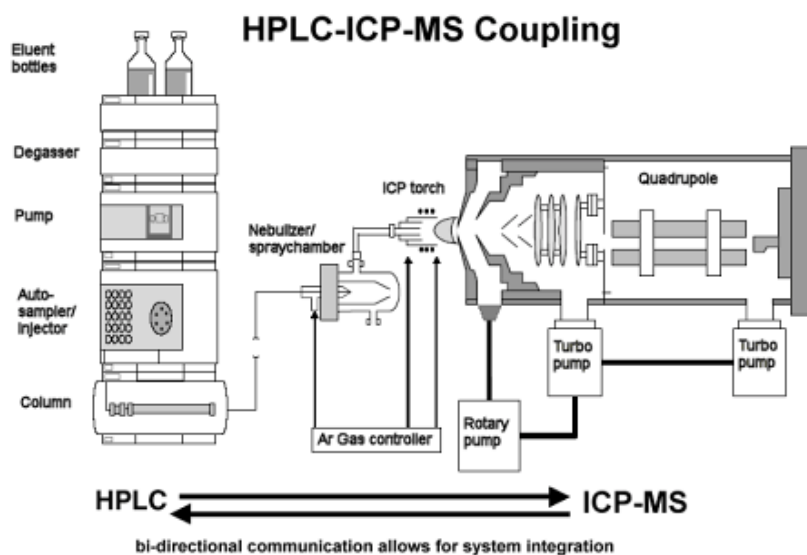


Figure 2.11 Example of HPLC-MS coupling

The component of the sample separated in the HPLC is vaporized and then ionized by inductive coupled plasma (ICP) or other techniques, to produce ions. The ions are separated according to their mass-to-charge ratio in an analyzer by electromagnetic fields. The ions are

detected by a quantitative method (e.g quadrupole) and the signal is processed into mass spectra.

In this work, HPLC–MS measurements were obtained on a Varian 212 series chromatograph equipped with Prostar 430 autosampler and MS-500 Ion Trap as detector. MS spectra were recorded in positive and in negative ion mode (50–2000 Da). The APCI ion source was used for lipid analysis while the ESI was used for phenolic and glucosinolates. Fragmentation of the main ionic species were obtained during the HPLC run by the turbo data depending scanning (tdds) function, yielding in fragmentation pattern of eluted compounds. As stationary phase Agilent Zorbax C-18 (2.1 × 150 mm) 3.5 μm was used. As mobile phases solvent A (water 0.1% formic acid) and solvent B (methanol) were utilized. The solvent gradient started at 80% A then decreased to 0% A over 30 min.

2.4.2 NMR

Nuclear magnetic resonance is a research technique that exploits magnetic properties of some atomic nuclei to determine physical and chemical properties of molecules in which they are contained. NMR make use of the phenomenon of nuclear magnetic resonance, the intramolecular magnetic field around an atom in a molecule changes the resonance frequency, revealing the electronic structure of a molecule. In H-NMR when a magnetic field is placed, ¹H (hydrogen isotope) nuclei absorb electromagnetic radiation at a frequency characteristic of the isotope. The resonant frequency, energy of absorption, and the intensity of the signal are proportional to the strength of the magnetic field. NMR spectra are unique and clearly determined. Different functional groups evidently distinguishable, furthermore identical functional groups with different neighbors substituents still give distinct signals.

The indicators used to assign a molecule are chemical shifts and spin-spin couplings. The variations of nuclear magnetic resonance frequencies of the same kind of nucleus (¹H), due to variations in the electron distribution, is called the chemical shift. In a magnetic field nuclei that possess a magnetic moment (nuclear spin) give rise to different levels of energy and resonance frequencies. The electron distribution of the same type of nucleus (¹H) depends on the local geometry (neighbors, bond length, angle between bonds...) and on the local magnetic field of each nucleus. This is exhibited in the variance of level of energy and the variance of resonance frequencies. Chemical shifts values are expressed in ppm.

Chemical shift is not the only indicator. Nuclei themselves possess a small magnetic field: they influence each other changing the energy and the resonance frequency. This is known as spin-spin coupling. The coupling constant is independent of magnetic field strength because it is caused by the magnetic field of another nucleus. Therefore it is quoted in hertz (frequency) and not ppm (chemical shift).

In this work NMR (1D and 2D) spectra were obtained on a Bruker Avance 400 spectrometer (Figure 2.12) operating at 400.14 MHz for ^1H and 100 MHz for ^{13}C . Spectra were obtained at 298 K using deuterated chloroform as solvent.



Figure 2.12: 400 MHz NMR spectrometer

Collected peaks from HPLC were evaporated to dryness in speedvac and the obtained residue was dissolved in 750 μL of CD_3OD . Spectra were obtained using standard pulse sequences of Topspin software.

CHAPTER 3

Results and discussion

The optimum values of the extraction parameters of the extraction have been investigated, and different co-solvents have been used for enhancing supercritical CO₂ extraction. The yields obtained have been compared to the solvent extraction technique. The extract have been analyzed to identify the desired compounds and their content.

3.1 Comparison of SCF extraction with Soxhlet extraction

Solvent extraction using Soxhlet apparatus has been performed in order to compare the results obtained with supercritical fluid extraction. SC-CO₂ extraction has been performed with the constant values of temperature, pressure, carbon dioxide flow rate using three different co-solvents : ethanol, methanol, water. Table 3.1. shows the conditions at which the preliminary tests have been performed.

Table 3.1 : SC-CO₂ parameters for comparison of different methods.

Pressure (bar)	300
Temperature (°C)	45
CO ₂ flow rate (kg/h)	0.3
Co-solvent conc. (wt %)	7

Soxhlet extraction has been carried out at 100 °C, using a mixture of methanol and water (70:30 v,v). The different yields obtained using both Soxhlet and SC-CO₂ extraction are compared in Figure 3.1. As can be seen, the extraction yield using an organic solvent in the Soxhlet apparatus is higher than that of the supercritical fluid extraction.

Supercritical carbon dioxide used without a co-solvent yields only 1.5%. Adding co-solvents leads to enhancement the extraction yield. In this study polar co-solvents were added since some of the components of interest are polar.

The results obtained with ethanol and methanol are similar 5.54% and 5.56%, respectively.

Higher amount of extract are obtained using water as co-solvent with respect to ethanol and methanol yields. This will be better explained in the following sections. At 45°C and 300 bar the yield obtained by supercritical fluid extraction using water as co-solvent is 21.71%.

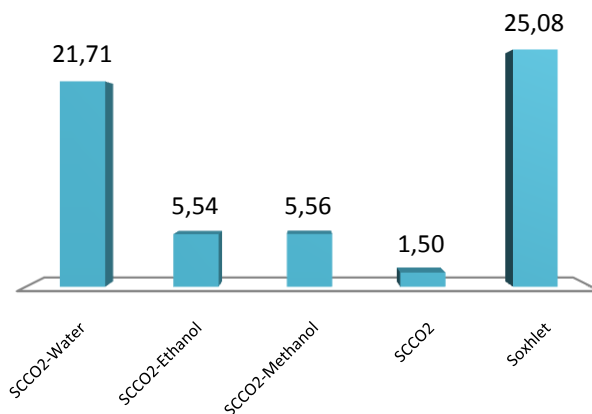


Figure 3.1: Comparison of the yields (%) obtained by SC-CO₂ with different co-solvents and by Soxhlet.

The enhancement of the amount of extract obtained with Soxhlet is probably related to the higher extraction temperature. The higher the temperature, the more cell walls are broken down, allowing the solvent to access to the compounds, solubilize them and extract them more easily.

3.2 Optimization of the extraction parameters using ethanol as co-solvent

In literature, ethanol is certainly the most often used co-solvent employed to increase the polarity of supercritical carbon dioxide. Since it is slightly polar, it can enhance the solvent power of the supercritical fluid allowing the extraction of polar compounds. Our first aim was to extract glucosinolates, which are polar compounds; for this reason ethanol was chosen as the co-solvent to be used in the first experimental test. The effect of the extraction parameters on the yield of the extraction was investigated. First, the influence of the CO₂ flow rate on the yield of the extraction was examined. Moreover, an optimum value of the ethanol dosage was found. Beside these, the influence of the pre-treatment on the yield of the extraction was confirmed. Finally, optimum values of the extraction temperature and pressure were achieved.

3.2.1 Effect of CO₂ flow rate on the yield of the extraction

In order to find the optimum value of the CO₂ flow rate, various experiments at different CO₂ flow rates were performed.

The other parameters were kept at constant values shown in the Table 3.2.

Table 3.2: Extraction parameters values

Pressure (bar)	300
Temperature (°C)	45
Co-solvent dosage (mL/min)	0.5

These values are considered as a reference from previous extraction experiments. Typical results are shown in Figure 3.2. There is an enhancement of the extraction yield while decreasing the flow rate of the SCCO₂ from 0.5 kg/h to 0.3 kg/h. Higher velocity leads to lower time contact of solvent with the particles and hence to lower yield.

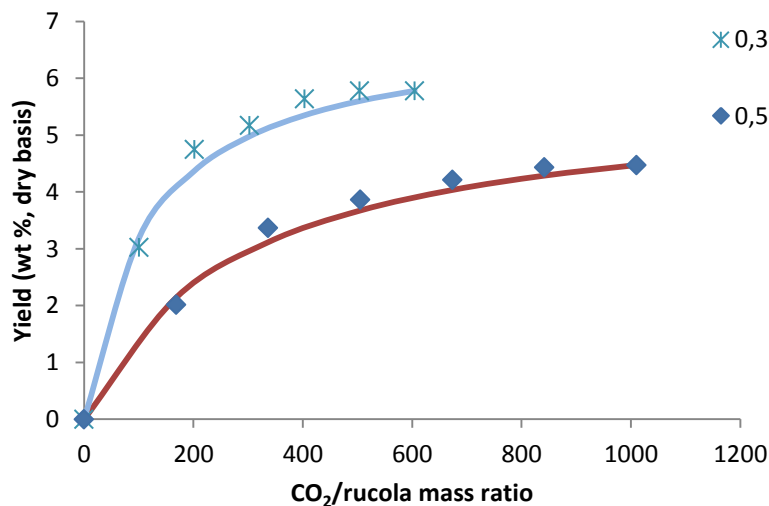


Figure 3.2: Effect of CO₂ flow rate on the extraction yield

According to literature ⁽³²⁾ the final yield can be estimated from the following correlation (3.1):

$$Y = k_s * a_s * V_t * \Delta c_m \quad (3.1)$$

Where k_s is the mass transfer coefficient (m/s); a_s the specific interfacial area (m^2/m^3); V_t the bed volume (m^3); and Δc_m the mean concentration gradient. The mass transfer coefficient, k_s can be calculated by a correlation with the Sherwood number (3.2)

$$Sh = k_s * d/D_{12} = 2 + 1.1 * Sc^{1/3} * Re^{0.6} \quad \text{for } 3 < Re < 3000 \quad (3.2)$$

Since an increasing of the flow rates leads to an increasing of the Reynolds number defined as (3.3)

$$Re = (v * d) / \nu \quad (3.3)$$

This should lead to an enhancement of the yield, because at the same extractor diameter, d , the velocity is increasing. However more CO_2 would be needed to extract the same quantity.

3.2.2 Optimization of the ethanol dosage

Since pure SCCO_2 has low solvent power for the substances, we want to extract a small amount of co-solvent was added. Ethanol was chosen, as it is a polar liquid and it is the most employed co-solvent in literature. The effect of the dosage of ethanol on the extraction yield was investigated. The values of the other extraction parameters were kept constant (Table 3.3):

Table 3.3: Extraction parameters values for the optimization of the ethanol dosage

Pressure (bar)	300
Temperature ($^{\circ}\text{C}$)	45
CO_2 flow rate (kg/h)	0.3

Extraction experiments were carried out with different values of ethanol dosage, varying dosage between 0.3 and 0.7 mL/min, with steps of 0.1 mL/min. Since the addition of co-solvent affects the solubility of the substances in the solvent, an increasing amount of ethanol should lead to increasing solubility, and increasing final yields.

The extraction curves obtained are shown in Figure 3.3. As can be seen, increasing the dosage of ethanol leads to increase of the slope of the linear part of the curve, that means higher solubility.

Passing from 0.3 to 0.4 mL/min clearly to increases the solubility and the yield. This trend is true also at 0.5 mL/min. However further increasing of the ethanol concentration does not lead to further advantages. The final yield seems to reach a maximum with 0.5 mL/min. Higher values of co-solvent amounts do not improve the yield.

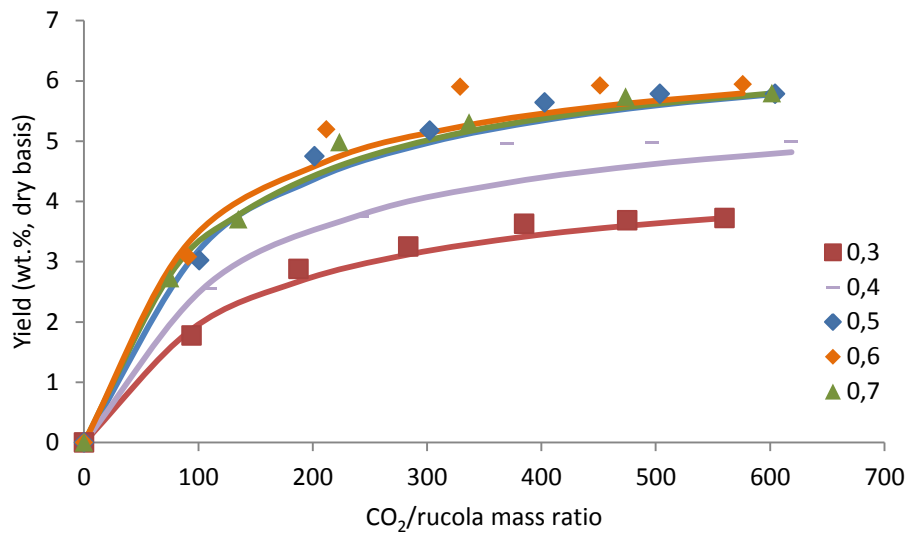


Figure 3.3: Effect of the ethanol dosage on the extraction yield

A comparison of the values of the final yields is shown in Figure 3.4

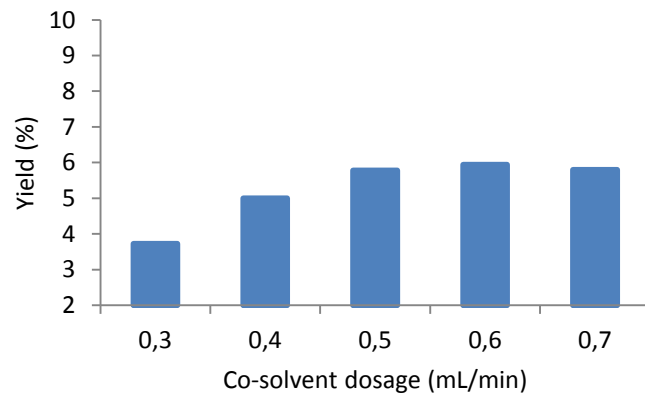


Figure 3.4: Comparison of the final yields

The optimum value of the ethanol dosage is furthermore confirmed if we compare the solubility data shown in Figure 3.5

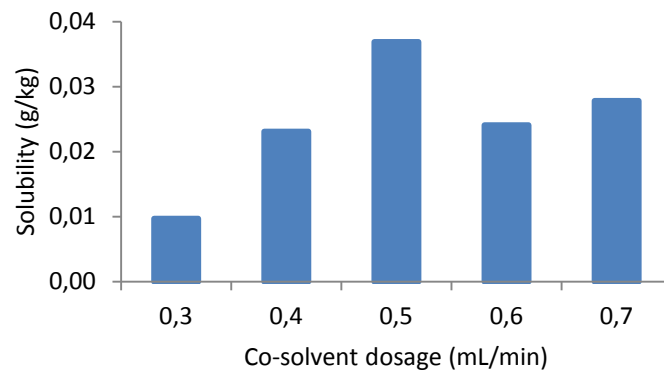


Figure 3.5: Solubility at different ethanol dosage

To sum up, the optimum value of the co-solvent dosage seems to be 0.5 mL/min (7 wt %), this may be due to that this amount of ethanol is solubilized in the SCCO₂ and brought inside the cell to the available soluble compounds. A larger amount of ethanol is not fully solubilized in SCCO₂ and therefore it is not able to access to the available substances inside the cells.

3.2.3 Effect of the pre-treatment on the yield of the extraction

The mechanism of transport in the solid phase proceeds in the following parallel and consecutive steps:

- The solvent is absorbed in the plant, swelling the cell structure and dissolving the soluble compounds
- The dissolved substances are transported to the outer surface by diffusion
- The dissolved substances are transported from the surface layer to the solvent

Particle size distribution and the initial location of the desired compounds in the solid matrix play important roles on the hydrodynamic of the solvent and the diffusion. For this reason a mechanical pre-treatment was performed to the dried leaves before the extraction experiments.

After being freeze-dried, the leaves were grinded with a laboratory pestle. The powder obtained was then filtered with a metallic sieve of 0.5 mm. It has been reported that the size of the particles should be in a range between 0.4 and 0.8 mm. Smaller particle sizes can cause channeling.⁽³³⁾

The main effect of this process is to increase a_v , the specific interfacial area (m_2/m_3). This leads directly to an enhancement of the yield as reported from the correlation (3.1). Moreover, the mechanical pre-treatment breaks the cell walls, this helps the diffusion process. In this

way the soluble compounds are directly available for the solvent that can easily dissolve and extract them.

The influence of the mechanical pre-treatment is shown in the following Figure 3.6.

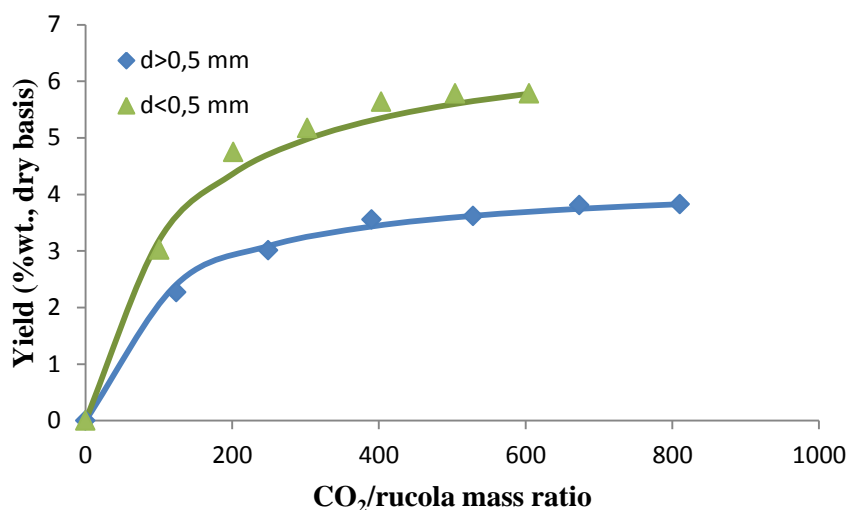


Figure 3.6: Influence of the pre-treatment on the extraction yield

As can be seen in Figure 3.6 a higher yield is reached in the pre-treated sample since the first part of the extraction curve (solubility limited), with a lower amount of solvent. The main effect is noticed in the following part of the extraction curve. Diffusion is related to the size of particles, the lower the size particle the faster the diffusion. The mechanism of transport in the solid phase shown previously is accelerated by regular particle size distribution, and especially the increasing of the interfacial area a_s . The “fresh” solvent can more easily access to the solid phase and being absorbed. Moreover diffusion from the inner to the outer surface is faster and the dissolved substance can more easily being transported from the surface layer into the solvent.

The result is that in a mechanical pre-treated sample the final yield is higher and the amount of solvent consumed is smaller than that of the sample without pre-treatment.

3.2.4 Optimization of the temperature on the extraction process

In order to find the optimum value of the extraction temperature, various experiments have been carried out at different temperatures. The other extraction parameters, kept constant, are shown in Table 3.4.

Table 3.4: Extraction parameters values for temperature optimization

Pressure (bar)	300
Ethanol dosage (mL/min)	0.5
CO ₂ flow rate (kg/h)	0.3

The extraction curves at different temperatures are shown in the Figure 3.7 .

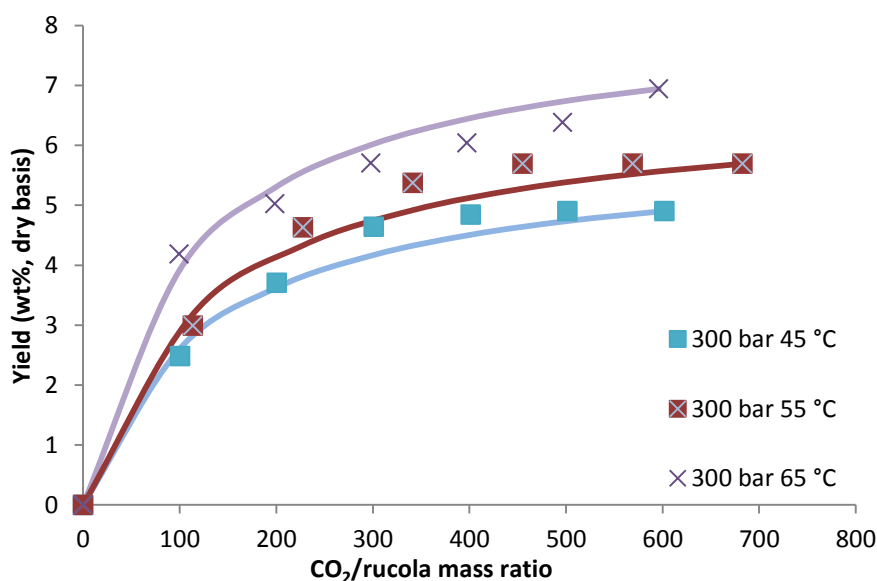


Figure 3.7: Optimization of the extraction temperature

Increasing the temperature leads to higher final yield values. Rising of temperature lead to decreasing of the density of supercritical fluid and an increasing of the vapor pressure of the solute. Since the pressure is at 300 bar the influence on the vapor pressure is superior to that of the decreasing of the density. For this reason increasing the temperature has a positive effect on the yield of the extraction. The upper limit of temperature is determined by the temperature of degradation of the desired compounds. For glucosinolates using supercritical CO₂, this is usually 70 °C⁽²⁴⁾, for flavonoids and lipids is 60°C^(25,29).

3.2.5 Optimization of the pressure on the extraction process

Pressure is the parameter that mostly effects the density, and so the yield of the supercritical extraction process. Increasing of the pressure always leads to increasing of the density, meaning an enhancement of the extraction yield. To confirm this concept experimental proofs have been performed at different pressures keeping constant the values of the other parameters (Table 3.5).

Table 3.5: Extraction parameters values for the optimization of extraction pressure

Temperature (°C)	45
CO ₂ flow rate (kg/h)	0.3
Ethanol dosage (mL/min)	0.5

The results obtained at different pressures are shown in Figure 3.8

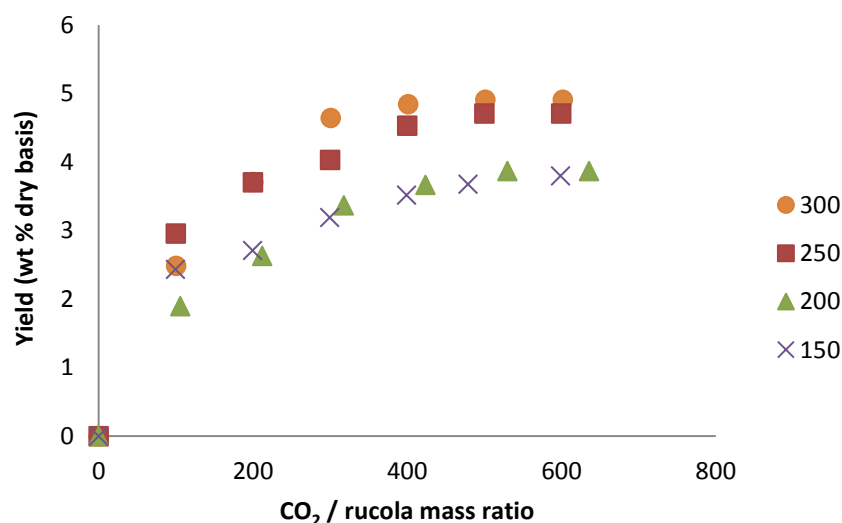


Figure 3.8: Optimization of the extraction pressure

Our results confirm that increasing the extraction pressure always leads to larger final yields. There is a slight enhancement of the yield from increasing the pressure from 150 bar to 200 bar. This improvement becomes more evident raising the pressure to 250 and 300 bar.

3.3 Optimization of the extraction parameters using water as co-solvent

Beside ethanol, water can be employed as co-solvent in supercritical CO₂ extraction (¹). Water and ethanol are physically similar and there are both used as co-solvent to allow to the supercritical CO₂ to solubilize also polar components. Experiments have been carried out in order to find an optimum value of the water dosage, extraction pressure and extraction temperature.

3.3.1 Optimization of the water dosage

The optimum dosage of water has been investigated. Experiments have been performed varying its value and keeping the other parameters at the constant values shown in Table 3.6

Table 3.6: Extraction parameters values for the optimization of the water dosage

Pressure (bar)	300
Temperature (°C)	65
CO ₂ flow rate (kg/h)	0.3

The water dosage was varied among 0.3 mL/min, 0.4 mL/min, 0.5 mL/min corresponding to respectively 6 wt %, 7 wt % and 10 wt% . The extraction curves are shown below (Figure 3.9).

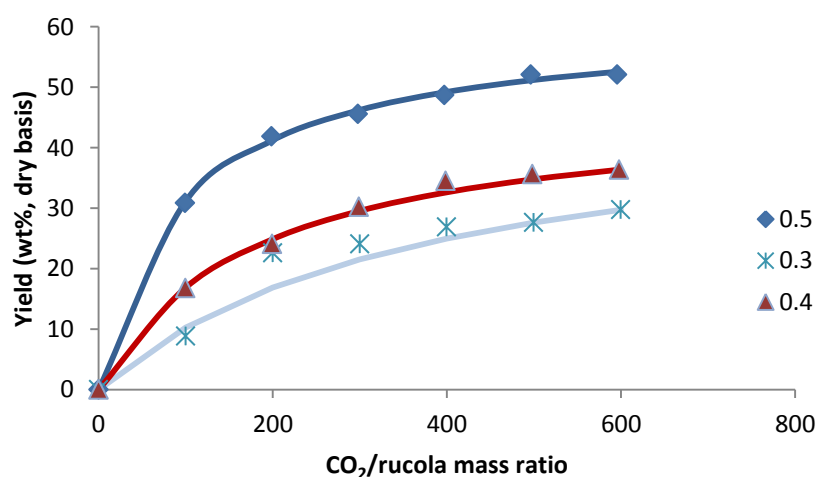


Figure 3.9: Optimization of the water dosage

The results shows clearly that increasing of water dosage leads to better yields.

Particularly, the result obtained with 0.5 mL/min of water was very high. However for the following experiments 0.4 mL/min was chosen as optimum value, since with a larger flow rates of water the system was blocked. This could be due to that the increase of co-solvent percentage may induce to the saturation of CO₂ with water, with consequent formation of two phases for the specific conditions of the system (³⁴).

3.3.2 Optimization of the temperature on the extraction process

The effect of the temperature on the extraction yield has been investigated. Temperature was varied among 45°C, 55°C, 65°C and 75°C. The other extraction parameters were kept at the constant values shown in Table 3.7.

Table 3.7: Extraction parameters values for the optimization of temperature

Pressure (bar)	300
Water dosage (mL/min)	0.4
CO ₂ flow rate (kg/h)	0.3

Extraction curves at different temperatures are shown in Figure 3.10.

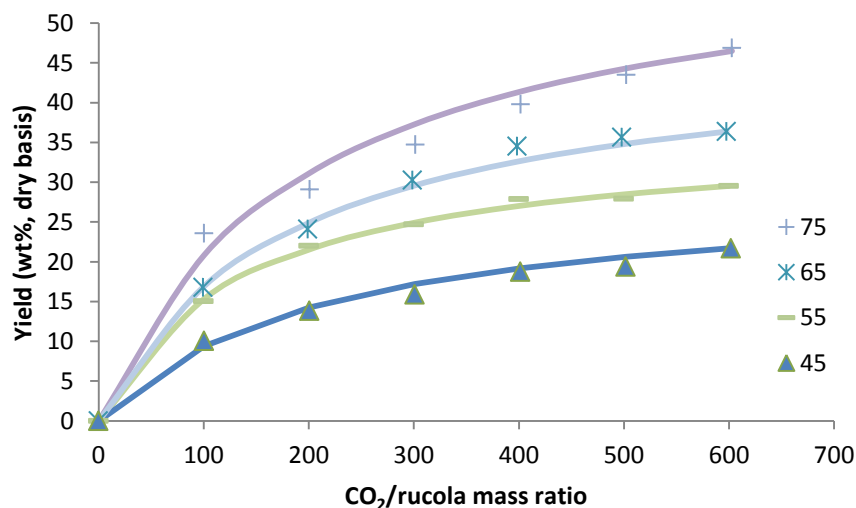


Figure 3.10: Optimization of the temperature

Temperature has an evident effect on the yield. Increasing of temperature leads to enhancement of both solubility and diffusivity, resulting in a higher final yield.

Since supercritical fluid extraction of the valuable compounds that we want extract are usually performed at 70 °C (glucosinolates), ⁽²⁴⁾ or 60 °C (flavonoids and lipids), ⁽²⁵⁾ and ⁽²⁹⁾ 65°C was chosen as an optimum value for the experiments, to avoid the degradation of the compounds.

3.3.3 Optimization of the pressure on the extraction process

In order to investigate the optimum value of the extraction pressure, supercritical CO₂ extraction has been performed at four different pressures ranged from 150 bar to 300 bar. The values of the other extraction parameters are shown in Table 3.8.

Table 3.8: Extraction parameters values for the optimization of pressure

Temperature (°C)	65
CO ₂ flow rate (kg/h)	0.3
Water dosage (mL/min)	0.4

The extraction curves are shown in Figure 3.11 .

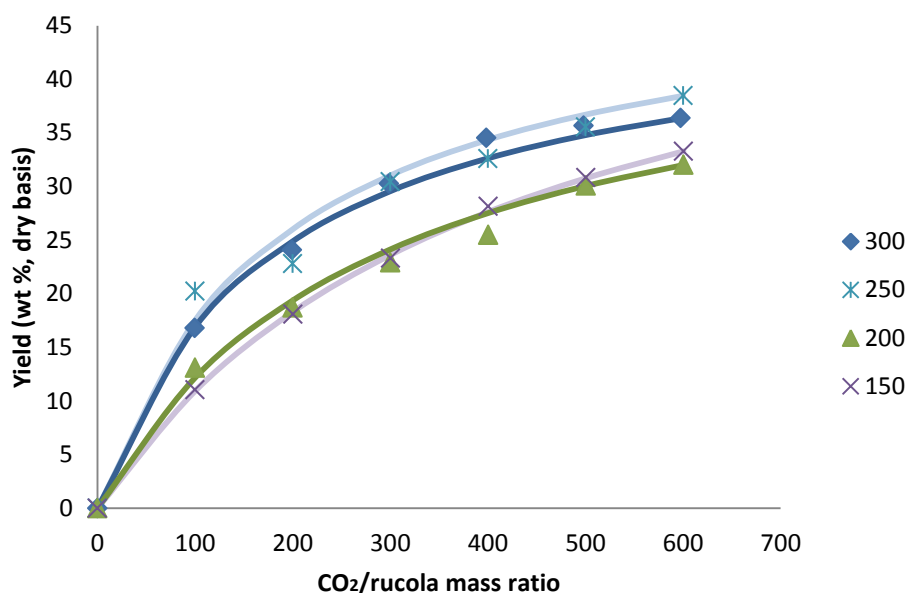


Figure 3.11: Optimization of the extraction pressure

The effect of increasing pressure on the extraction yield is not as evident as that of temperature. Increasing pressure leads to higher the density of the supercritical fluid, which that should always lead to an enhancement of the yield of the extraction. This enhancement is clearly shown if we compare the yield at 150 bar with that of 300 bar. However, the experimental values at 200 bar are not far from those of 150 bar, moreover the final value is even smaller. The same behavior is represented from the curve at 250 bar with that of 300 bar, and again the final value of 250 bar is higher than that of 300. What we can conclude concerning these experiments, is that increasing of pressure does not influence primarily the yield of the extraction. Similar data have been found in literature when water was used as co-solvent ⁽³⁴⁾.

3.4 Comparison between three different co-solvents

Three different co-solvents have been employed in the supercritical fluid extraction: ethanol, methanol and water. These are physically similar as they are polar protic solvents ⁽³⁵⁾. They are compared in Table 3.9.

Table 3.9: Comparison of the physical properties of the solvents

Solvent	Chemical Formula	Boiling point	Dielectric constant	Density	Dipole moment (D)
Ethanol (EtOH)	CH ₃ -CH ₂ -OH	79 °C	30	0.789 g/ml	1.69 D
Methanol (MeOH)	CH ₃ -OH	65 °C	33	0.791 g/ml	1.70 D
Water	H-O-H	100 °C	80	1.000 g/ml	1.85 D

Ethanol and methanol are very similar in terms of dielectric constant, density and dipole moment. Water has a superior value of density, dipole moment and especially of dielectric constant.

Supercritical CO₂ has been performed using these chemicals as co-solvents at the same conditions, shown in Table 3.10.

Table 3.10: Extraction parameters values for the co-solvents comparison

Pressure (bar)	300
Temperature (°C)	45
CO ₂ flow rate (kg/h)	0.3
Co-solvent dosage (wt %)	0.7

The comparison of the different yields is shown in the Figure 3.12.

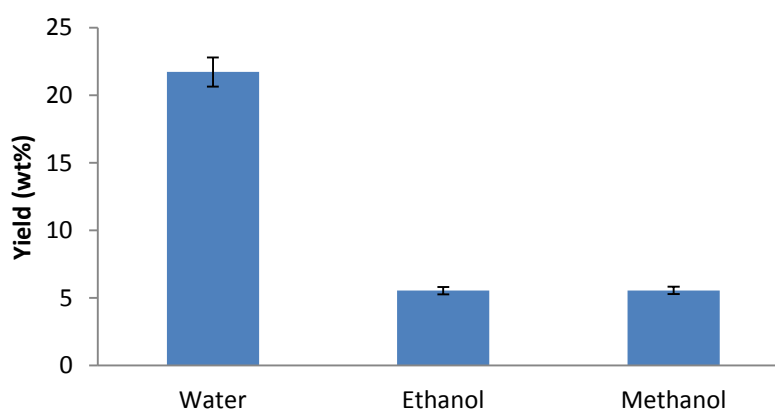


Figure 3.12: Extraction yield with different co-solvent

The results show that the extraction yield obtained with ethanol and methanol are similar, 5.54 ± 0.245 % and 5.6 ± 0.06 , respectively. The most evident data is the high yield achieved with water (21.71 ± 0.61 %) in comparison with ethanol and methanol.

3.5 Effect of the extraction conditions on the *Eruca sativa* extract composition

Samples of the extracts of each experiment test have been analyzed in order to identify qualitatively and quantitatively glucosinolates, flavonoids, and lipids present in them. The results of each category of compounds is shown below.

3.5.1 Glucosinolates

The glucosinolates content was analyzed twice for each sample. The tables reported below show the media and the standard deviation of the two values.

First, glucosinolates content of the extracts obtained using different co-solvents was investigated. As shown Table 3.11, no glucosinolates were extracted with pure CO₂ and using ethanol as co-solvent, and a very small quantity (0.3 mg/g) was extracted using methanol as co-solvent. The highest content of glucosinolates, 7.3 mg/g, was found in the extracted obtained by SCCO₂ using water as co-solvent. Hence, the effect of the SCCO₂ operating conditions on the glucosinolates content when water is used as co-solvent was studied.

Table 3.11: Glucosinolates composition (mg/g) of *Eruca sativa* extract obtained by SCCO₂ using different co-solvents.

Co-solvent	Water	Methanol	Ethanol	None
GL Erucin	0.85±0.26	0.00±0.00	0.00±0.00	0.00±0.00
GL Rafanin	0.30±0.03	0.00±0.00	0.00±0.00	0.00±0.00
DMB-GLS	5.74±0.28	0.30±0.02	0.00±0.00	0.00±0.00
GL Cheirolin	0.00±0.00	0.00±0.00	0.00±0.00	0.00±0.00
GL Sativin	0.37±0.02	0.00±0.00	0.00±0.00	0.00±0.00
NeoGlBrassicin	0.00±0.00	0.00±0.00	0.00±0.00	0.00±0.00
GlBrassicin	0.00±0.00	0.00±0.00	0.00±0.00	0.00±0.00
Total	7.25±0.03	0.30±0.02	0.00±0.00	0.00±0.00

The effect of the temperature of supercritical fluid extraction on the glucosinolate composition is shown in Table . The extractions were carried out at 75°C, 65°C and 55°C, maintaining constant the other parameters (300 bar, 0.4 mL/min of water). As shown Table 3.12 , the highest glucosinolate content (7.3 mg/g) was found on the extract obtained at 65 °C. When the extraction was performed at 75°C, no glucosinolates were found on the sample. This can be due to the degradation of the compounds at high temperatures. At 55°C a small quantity of glucosinolates was extracted with respect to the 65°C sample.

Table 3.12 : Glucosinolates composition (mg/g) of *Eruca sativa* extract obtained by SCCO₂ at different temperatures.

Temperature (°C)	75°C	65°C	55°C
GL Erucin	0.00±0.00	0.85±0.26	0.32±0.09
GL Rafanin	0.00±0.00	0.30±0.03	0.18±0.03
DMB-GLS	0.00±0.00	5.74±0.28	0.61±0.23
GL Cheirolin	0.00±0.00	0.00±0.00	0.08±0.00
GL Sativin	0.00±0.00	0.37±0.02	0.00±0.00
NeoGIBrassicin	0.00±0.00	0.00±0.00	0.00±0.00
GIBrassicin	0.00±0.00	0.00±0.00	0.00±0.00
Total	0.00±0.00	7.25±0.03	1.19±0.30

Different tests were carried out at different pressures maintaining constant the other parameters (65°C, 0.4 mL/min of water) with the aim of studying the effect of the pressure on the glucosinolates composition of the extract. As shown in Table 3.13, the higher the pressure, the higher the glucosinolates content on the extract. Probably, at 300 bar, the enzyme myrosinase is deactivated, whereas lower pressures are not high enough to deactivate it.

Table 3.13: Glucosinolates composition (mg/g) of *Eruca sativa* extract obtained by SCCO₂ at different pressures.

Pressure (bar)	300	250	200	150
GL Erucin	0.85±0.26	0.24±0.03	0.22±0.01	0.26±0.03
GL Rafanin	0.30±0.03	0.00±0.00	0.00±0.00	0.20±0.01
DMB-GLS	5.74±0.28	1.59±0.91	0.54±0.36	0.00±0.00
GL Cheirolin	0.00±0.00	0.00±0.00	0.00±0.00	0.00±0.00
GL Sativin	0.37±0.02	0.00±0.00	0.00±0.00	0.00±0.00
NeoGIBrassicin	0.00±0.00	0.00±0.00	0.00±0.00	0.00±0.00
GIBrassicin	0.00±0.00	0.00±0.00	0.00±0.00	0.00±0.00
Total	7.25±0.03	1.83±0.94	0.76±0.35	0.45±0.02

The effect of the co-solvent dosage on the glucosinolates composition is shown in Table 3.14. The highest value, 7.3 mg/g, was obtained using 0.4 mL/min. As explained in the previous sections, with 0.5 mL/min, the saturation of CO₂ with water with consequently formation of two phases for the specific conditions of the system could have been taken place. It is also noted that 0.3 mL/min of water is not enough to extract the glucosinolates from *Eruca sativa* leaves.

Table 3.14: Glucosinolates composition (mg/g) of *Eruca sativa* extract obtained by SCCO₂ with different co-solvent dosages.

Co-solvent dosage (mL/min)	0.3	0.4	0.5
GL Erucin	0.11±0.04	0.85±0.26	0.00
GL Rafanin	0.00±0.00	0.30±0.03	0.72
DMB-GLS	0.00±0.00	5.74±0.28	0.35
GL Cheirolin	0.00±0.00	0.00±0.00	0.00
GL Sativin	0.00±0.00	0.37±0.02	0.00
NeoGlBrassicin	0.00±0.00	0.00±0.00	0.00
GlBrassicin	0.00±0.00	0.00±0.00	0.00
Total	0.11±0.04	7.25±0.03	1.07

Table 3.15 shows the results of the glucosinolates analysis from the samples extracted both with and without mechanical pre-treatment at 300 bar, 65 °C and 0.4 mL/min of water. Contrary to expectations, the highest glucosinolates content was extracted when the diameters of the particles were higher. It can be due to the fact that after the first milling and freeze-dried, the particles are small enough to allow the solvent and co-solvent to penetrate inside and extract the compounds.

Table 3.15: Glucosinolates composition (mg/g) of *Eruca sativa* extract obtained by SCCO₂ both with and without mechanical pre-treatment.

Particle diameter	< 0.5 mm	> 0.5 mm
GL Erucin	0.85±0.26	1.08±0.10
GL Rafanin	0.30±0.03	0.38±0.07
DMB-GLS	5.74±0.28	9.47±0.96
GL Cheirolin	0.00±0.00	0.00±0.00
GL Sativin	0.37±0.02	0.80±0.07
NeoGlBrassicin	0.00±0.00	0.00±0.00
GlBrassicin	0.00±0.00	0.00±0.00
Total	7.25±0.03	11.74±1.00

Glucosinolates composition of the extracts obtained by two different methods was also compared. Table 3.16 shows the comparison between the results obtained by SCCO₂ using water as co-solvent in the best conditions (65°C, 300 bar, 0.4 ml/min of co-solvent, without mechanical pre-treatment) and the composition of the extract obtained by Soxhlet at 100 °C. It is noted that the total content of glucosinolates is much higher when SCCO₂ is applied. This can be due to the high temperatures achieved with Soxhlet, that could have degraded the valuable compounds.

Table 3.16 : Glucosinolates composition (mg/g) of *Eruca sativa* extract obtained by SCCO₂ and Soxhlet extraction method.

Method	SCCO ₂	Soxhlet
GL Erucin	1.08±0.10	0.00±0.00
GL Rafanin	0.38±0.07	0.09±0.05
DMB-GLS	9.47±0.96	3.13±0.25
GL Cheirolin	0.00±0.00	0.04±0.00
GL Sativin	0.80±0.07	0.31±0.08
NeoGlBrassicin	0.00±0.00	0.00±0.00
GlBrassicin	0.00±0.00	0.00±0.00
Total	11.74±1.00	3.57±0.28

3.5.2 Phenols

The phenols content was analyzed four times for each sample. The tables reported below show the media and the standard deviation of the four values.

First, phenols content of the samples extracted using different co-solvents was analyzed. As shown Table 3.17, no phenolic compounds were extracted with pure CO₂, and very small traces were extracted using ethanol and methanol as co-solvents. The highest content of glucosinolates, 1.42 mg/g, was found in the extracted obtained by SCCO₂ using water as co-solvent. Therefore, the effect of the SCCO₂ operating conditions on the phenols content when water is used as co-solvent was investigated.

Table 3.17: Phenols composition (mg/g) of *Eruca sativa* extract obtained by SCCO₂ using different co-solvents

Co-solvent	Water	Methanol	Ethanol	None
Quinic acid	0.07±0.01	0.00±0.00	0.00±0.00	0.00±0.00
Quercetin-3-(2-feruloyl-glucoside)-3'-(6-feruloylglucoside)-4'glucoside	0.00±0.00	0.00±0.00	0.00±0.00	0.00±0.00
Quercetin-3,4'-diglucoside-3'(6-sinapoyl-glucoside)	0.16±0.01	0.06±0.00	0.00±0.00	0.00±0.00
Rutin	0.04±0.00	0.00±0.00	0.00±0.00	0.00±0.00
Leucodelphynidin	0.46±0.01	0.09±0.00	0.13±0.01	0.00±0.00
Q-acetil-sinapoyl-diglucoside	0.07±0.00	0.03±0.03	0.00±0.00	0.00±0.00
Quercetin(Sinapoyl-glucoside)(sinapoyl-glucoside)-glucoside	0.22±0.01	0.06±0.00	0.07±0.00	0.00±0.00
Quercetin(Sinapoyl-glucoside)	0.04±0.00	0.00±0.00	0.00±0.00	0.00±0.00
Quercetin	0.05±0.00	0.00±0.00	0.00±0.00	0.00±0.00
Kaempferol	0.04±0.00	0.00±0.00	0.00±0.00	0.00±0.00
Isoramnetin	0.04±0.00	0.00±0.00	0.00±0.00	0.00±0.00
Procatequic acid glucoside	0.05±0.00	0.00±0.00	0.00±0.00	0.00±0.00
Quercitin diglucoside	0.16±0.15	0.03±0.03	0.00±0.00	0.00±0.00
Total	1.42±0.18	0.28±0.01	0.19±0.01	0.00±0.00

The effect of the temperature of supercritical fluid extraction on the phenols composition is shown in Table 3.18. The compositions of the extract at 75°C, 65°C, 55°C and 45°C, maintaining constant the other parameters (300 bar, 0.4 mL/min of water) are reported. As shown Table 3.18, the higher the temperature, the higher the phenolic content. A total phenols content of 1.48 mg/g was found on the extract obtained at 75 °C. Hence, at 75°C no degradation of the phenolic compounds occur.

Table 3.18: Phenols composition (mg/g) of Eruca sativa extract obtained by SCCO₂ at different temperatures.

Temperature (°C)	75	65	55	45
Quinic acid	0.00±0.00	0.07±0.01	0.08±0.02	0.07±0.05
Quercetin-3-(2-feruloyl-glucoside)-3'-(6-feruloylglucoside)-4'glucoside	0.07±0.00	0.00±0.00	0.02±0.03	0.00±0.00
Quercetin-3,4'-diglucoside-3'(6-sinapoyl-glucoside)	0.11±0.02	0.16±0.01	0.14±0.03	0.08±0.02
Rutin	0.03±0.04	0.04±0.00	0.02±0.03	0.00±0.00
Leucodelphinidin	0.40±0.03	0.46±0.01	0.29±0.03	0.12±0.09
Q-acetil-sinapoyl-diglucoside	0.12±0.01	0.07±0.00	0.07±0.05	0.06±0.01
Quercetin(Sinapoyl-glucoside)(sinapoyl-glucoside)-glucoside	0.10±0.01	0.22±0.01	0.09±0.04	0.06±0.01
Quercetin(Sinapoyl-glucoside)	0.21±0.02	0.04±0.00	0.06±0.01	0.09±0.02
Quercetin	0.26±0.04	0.05±0.00	0.10±0.02	0.07±0.05
Kaempferol	0.08±0.01	0.04±0.00	0.04±0.03	0.04±0.00
Isoramnetin	0.09±0.00	0.04±0.00	0.06±0.00	0.05±0.00
Procatequic acid glucoside	0.00±0.00	0.05±0.00	0.02±0.03	0.00±0.00
Quercitin diglucoside	0.00±0.00	0.16±0.15	0.07±0.01	0.00±0.00
Total	1.48±0.13	1.42±0.18	1.07±0.08	0.64±0.18

Different experiments were carried out at different pressures maintaining the other parameters constant (65°C, 0.4 mL/min of water) with the aim of studying the effect of the pressure on the phenols composition of the extract. As shown in Table 3.19, the higher the pressure, the higher the glucosinolates content on the extract, except in the case of extraction at 150 bar. Nevertheless, the sample with the highest phenolic content, 1.42 mg/g, was extracted at the highest pressure, 300 bar.

Table 3.19: Phenols composition (mg/g) of *Eruca sativa* extract obtained by $SCCO_2$ at different pressures.

Pressure (bar)	300	250	200	150
Quinic acid	0.07±0.01	0.17±0.04	0.11±0.04	0.19±0.04
Quercetin-3-(2-feruloyl-glucoside)-3'-(6-feruloylglucoside)-4'glucoside	0.00±0.00	0.00±0.00	0.00±0.00	0.00±0.00
Quercetin-3,4'-diglucoside-3'(6-sinapoyl-glucoside)	0.16±0.01	0.14±0.02	0.13±0.03	0.16±0.03
Rutin	0.04±0.00	0.00±0.00	0.00±0.00	0.00±0.00
Leucodelphinidin	0.46±0.01	0.31±0.03	0.28±0.03	0.28±0.04
Q-acetil-sinapoil-diglucoside	0.07±0.00	0.09±0.02	0.09±0.01	0.10±0.01
Quercetin(Sinapoyl-glucoside)(sinapoyl-glucoside)-glucoside	0.22±0.01	0.08±0.01	0.08±0.01	0.12±0.02
Quercetin(Sinapoyl-glucoside)	0.04±0.00	0.11±0.01	0.08±0.01	0.11±0.01
Quercetin	0.05±0.00	0.16±0.02	0.14±0.02	0.14±0.02
Kaempferol	0.04±0.00	0.07±0.00	0.06±0.00	0.08±0.00
Isoramnetin	0.04±0.00	0.08±0.00	0.07±0.01	0.08±0.00
Procatequic acid glucoside	0.05±0.00	0.00±0.00	0.00±0.00	0.00±0.00
Quercitin diglucoside	0.16±0.15	0.00±0.00	0.00±0.00	0.00±0.00
Total	1.42±0.18	1.23±0.13	1.04±0.11	1.26±0.14

The effect of the co-solvent dosage on the phenols composition is shown in Table 3.20. The highest value, 1.42 mg/g, was obtained using 0.4 mL/min, as in the case of glucosinolates.

Table 3.20 : Phenols composition (mg/g) of *Eruca sativa* extract obtained by $SCCO_2$ with different co-solvent dosages.

Co-solvent dosage (mL/min)	0.5	0.4	0.3
Quinic acid	0.00±0.00	0.07±0.01	0.10±0.03
Quercetin-3-(2-feruloyl-glucoside)-3'-(6-feruloylglucoside)-4'glucoside	0.00±0.00	0.00±0.00	0.00±0.00
Quercetin-3,4'-diglucoside-3'(6-sinapoyl-glucoside)	0.07±0.01	0.16±0.01	0.14±0.02
Rutin	0.01±0.02	0.04±0.00	0.00±0.00
Leucodelphinidin	0.48±0.06	0.46±0.01	0.29±0.04
Q-acetil-sinapoil-diglucoside	0.07±0.01	0.07±0.00	0.08±0.01
Quercetin(Sinapoyl-glucoside)(sinapoyl-glucoside)-glucoside	0.08±0.02	0.22±0.01	0.08±0.02
Quercetin(Sinapoyl-glucoside)	0.13±0.02	0.04±0.00	0.14±0.02
Quercetin	0.25±0.10	0.05±0.00	0.16±0.02
Kaempferol	0.07±0.02	0.04±0.00	0.04±0.03
Isoramnetin	0.08±0.02	0.04±0.00	0.07±0.00
Procatequic acid glucoside	0.00±0.00	0.05±0.00	0.00±0.00
Quercitin diglucoside	0.08±0.02	0.16±0.15	0.00±0.00
Total	1.31±0.16	1.42±0.18	1.11±0.13

Table 3.21 shows the results of the phenols analysis from the samples extracted both with and without mechanical pre-treatment at 300 bar, 65 °C and 0.4 mL/min of water. In this case, the highest phenols content was extracted when the diameters of the particles were smaller, as expected.

Table 3.21 : Phenols composition (mg/g) of Eruca sativa extract obtained by SCCO₂ both with and without mechanical pre-treatment.

Particle diameter	< 0.5 mm	> 0.5 mm
Quinic acid	0.07±0.01	0.13±0.08
Quercetin-3-(2-feruloyl-glucoside)-3'-(6-feruloylglucoside)-4'glucoside	0.00±0.00	0.00±0.00
Quercetin-3,4'-diglucoside-3'(6-sinapoyl-glucoside)	0.16±0.01	0.09±0.03
Rutin	0.04±0.00	0.05±0.01
Leucodelphynidin	0.46±0.01	0.30±0.04
Q-acetil-sinapoil-diglucoside	0.07±0.00	0.06±0.01
Quercetin(Sinapoyl-glucoside)(sinapoyl-glucoside)-glucoside	0.22±0.01	0.08±0.03
Quercetin(Sinapoyl-glucoside)	0.04±0.00	0.01±0.02
Quercetin	0.05±0.00	0.02±0.05
Kaempferol	0.04±0.00	0.01±0.02
Isoramnetin	0.04±0.00	0.01±0.02
Procatequic acid glucoside	0.05±0.00	0.05±0.05
Quercitin diglucoside	0.16±0.15	0.07±0.02
Total	1.42±0.18	0.89±0.13

Phenols composition of the extracts obtained by two different methods was compared. Table 3.22 shows the comparison between the results obtained by SCCO₂ using water as co-solvent at 65°C, 300 bar, 0.4 ml/min of co-solvent without mechanical pre-treatment, and the composition of the extract obtained by Soxhlet at 100 °C. As in the content of glucosinolates, the phenols content is much higher when SCCO₂ is applied. Once again, this can be due to the high temperatures achieved with Soxhlet, that could have degraded the valuable compounds.

Table 3.22 : Phenols composition (mg/g) of *Eruca sativa* extract obtained by SCCO₂ and Soxhlet extraction methods.

Method	SCCO ₂	Soxhlet
Quinic acid	0.07±0.01	0.00±0.00
Quercetin-3-(2-feruloyl-glucoside)-3'-(6-feruloylglucoside)-4'glucoside	0.00±0.00	0.00±0.00
Quercetin-3,4'-diglucoside-3'(6-sinapoyl-glucoside)	0.16±0.01	0.00±0.00
Rutin	0.04±0.00	0.00±0.00
Leucodelphinidin	0.46±0.01	0.11±0.03
Q-acetil-sinapoil-diglucoside	0.07±0.00	0.00±0.00
Quercetin(Sinapoyl-glucoside)(sinapoyl-glucoside)-glucoside	0.22±0.01	0.02±0.00
Quercetin(Sinapoyl-glucoside)	0.04±0.00	0.00±0.00
Quercetin	0.05±0.00	0.00±0.00
Kaempferol	0.04±0.00	0.00±0.00
Isoramnetin	0.04±0.00	0.00±0.00
Procatequic acid glucoside	0.05±0.00	0.03±0.00
Quercitin diglucoside	0.16±0.15	0.00±0.00
Total	1.42±0.18	0.16±0.04

3.5.3 Lipids

The lipids content was analyzed twice for each sample. Table 3.23 shows the media and the standard deviation of the two values. The samples were obtained by pure SCCO₂ and by SCCO₂ using water as-solvent at 300 bar and 45 °C. As expected, the sample extracted by pure SCCO₂ has a high content of lipids (338.0 mg/g), very rich in unsaturated fatty acids. However, the sample extracted using water as co-solvent has only very small traces of lipids.

Table 3.23: Lipids composition (mg/g) of *Eruca sativa* extract obtained by pure SCCO₂ and by SCCO₂ using water as-solvent.

Co-solvent	None	Water
MAG(Ln)	4.36±0.38	0.00
TG(LnLnSt)	183.8±12.10	0.00
TG(LnLnLn)	102.42±8.15	0.00
TG(LLnLn)	1.09±0.01	0.04
TG(linolenico)	9.56±0.04	0.02
TG(PLn)	0.57±0.04	0.00
TG(linolenic)	6.38±0.19	0.00
TG(LnLL)	0.94±0.01	0.00
TG(arachidic ac)	6.84±8.33	0.00
DG_PP	0.60±0.08	0.00
DG_(linolenic)	2.76±0.59	0.00
DG_CaCa	1.45±0.06	0.00
Not identified lipid	8.20±0.30	0.00
Not identified lipid	8.38±0.89	0.00
Not identified lipid	0.64±0.00	0.00
Total	338.01±12.65	0.06

CHAPTER 4

Economical evaluation of an industrial scale application

A conceptual design of an industrial scale application of the of the supercritical CO₂ extraction process has been proposed. Aspen plus software has been used for the design. An economical evaluation of the process has been performed in order to verify the economic feasibility of the scale up of this process.

4.1 Simulation model

Starting from the laboratory supercritical extraction plant, a conceptual design of an industrial scale application has been proposed. The hierarchical approach of Douglas (³⁶) has been followed for the design. The block diagram of the process is shown in Figure 4.1.

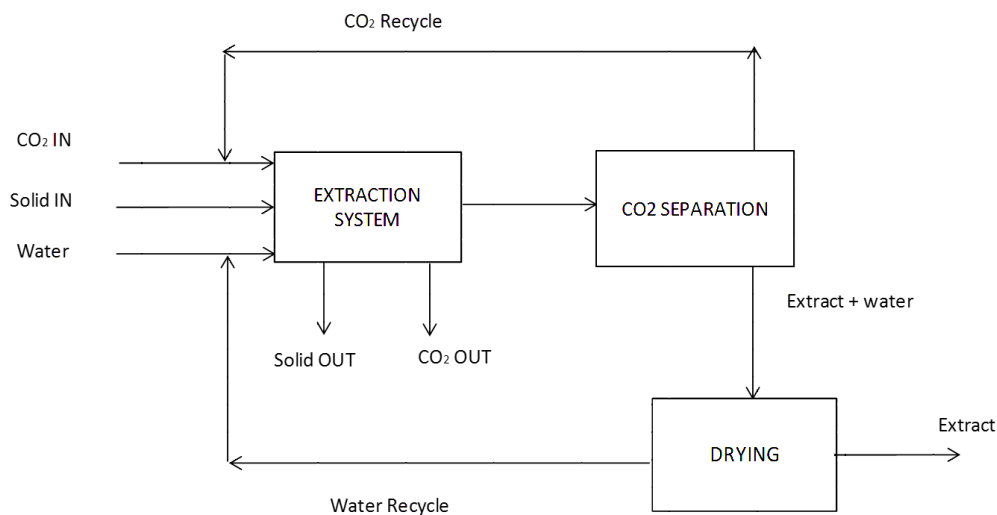


Figure 4.1: Block Flow Diagram of the process

In the laboratory plant the extraction is operated in batch mode, since there is only one extractor. However, adding another extractor in parallel allows operating in a semi-continuous

mode. For this hypothesis of conceptual design, the process is supposed to be operated in a continuous mode.

Process inlets are the solid material to be extracted (Solid IN), the fresh carbon dioxide (CO₂ IN) and the co-solvent to be added (Water). The outlets are the stream of the extract (Extract), the solid raffinate (Solid Out), and the loss of carbon dioxide remained after the extraction and inevitably lost during opening and refilling the extractor vessel. Two are the main blocks of the process: the extraction system and the carbon dioxide separator. The extraction system is supposed to include three supercritical extractors operating in parallel. The carbon dioxide separator assumed as a flash unit, which allows to separate carbon dioxide by depressurization. Another separation step has to be included in the system, since the water used as co-solvent has to be separated to recover the extract. This separation step is supposed to be a drying unit, and water is assumed to be completely recycled.

As basis for the calculations the amount of solid feed is set to 100 kg/h. The extraction curve obtained at 250 bar and 65 °C was chosen as reference.

$$Y = \left(\frac{50.57 * X}{188.94 + X} \right) \quad (4.1)$$

Where $Y = \text{flow rate of the extract} / \text{flow rate of solid} * 100$, $X = \text{mass of carbon dioxide} / \text{mass of solid}$.

X was fixed at 300 so that the flow rate of the extract should be 31.03 kg/h and the solid out is 68.97 kg/h. According to the experimental results the initial amount of water inlet is 7 wt % of that of carbon dioxide.

The loss of carbon dioxide has been evaluated from the porosity of the solid bed in the laboratory extractor. The volume of the lab extractor is $V_r = 2.6 * 10^{-6} \text{ m}^3$; the mass of solid put in is $m_s = 0.5 * 10^{-3} \text{ kg}$, so that the apparent density of the solid is $\rho_a = 190 \text{ kg/m}^3$. The real density of the solid has been calculated experimentally from a volumetric measure, finding $\rho_s = 1554 \text{ kg/m}^3$, meaning that the real volume occupied by the solid is $V_s = 3.2 * 10^{-7} \text{ m}^3$. The rest of the volume of the extractor $V_r - V_s = 2.28 * 10^{-6} \text{ m}^3$ is occupied by supercritical CO₂. The density of carbon dioxide at 250 bar 809 kg/m³, that leads to $1.8 * 10^{-3} \text{ kg}$ of carbon dioxide which are in the reactor and are lost when it is opened. The ratio mass of carbon dioxide/mass of solid in the laboratory extractor is 3.6. Hence, the loss of carbon dioxide in the process with a feed of 100 kg/h is CO₂ OUT= 360 kg/h.

To extract 100 kg/h with a residence time of 1 h, the total required volume is 530 L. Extraction is assumed to be carried out in three extractors in parallel of 360 L. A ratio of $\text{length/diameter} = 4$ has been considered (³³), obtaining, $\text{diameter} = 0.48 \text{ m}$ and $\text{length} = 2 \text{ m}$.

4.1.1 Aspen Plus

The software used for the design was Aspen Plus V 7.3. The components chosen were all conventional components, shown in Table 4.1.

Table 4.1: Components considered in the process

CO ₂	Conventional	Carbon dioxide
H ₂ O	Conventional	Water
OIL	Conventional	Linoleic acid
NOEXT	Conventional	Cellulose

The extract is approximated with the conventional component oil, and the part that cannot be extracted is approximated with cellulose.

SRK was chosen as property calculation method. The thermodynamic consistence of the chosen method has been evaluated by comparing data obtained from SRK with experimental data. For instance, the density of carbon dioxide has been calculated at different pressures and temperatures with the Equation of Bender (³⁷) and SRK. The results are compared in Figure 4.2-4.5.

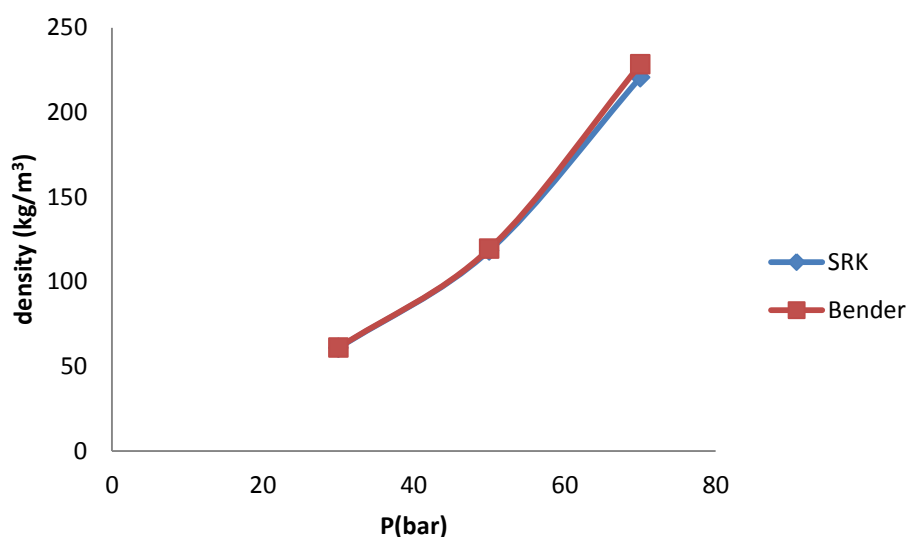


Figure 4.2: Carbon dioxide density at 32°C

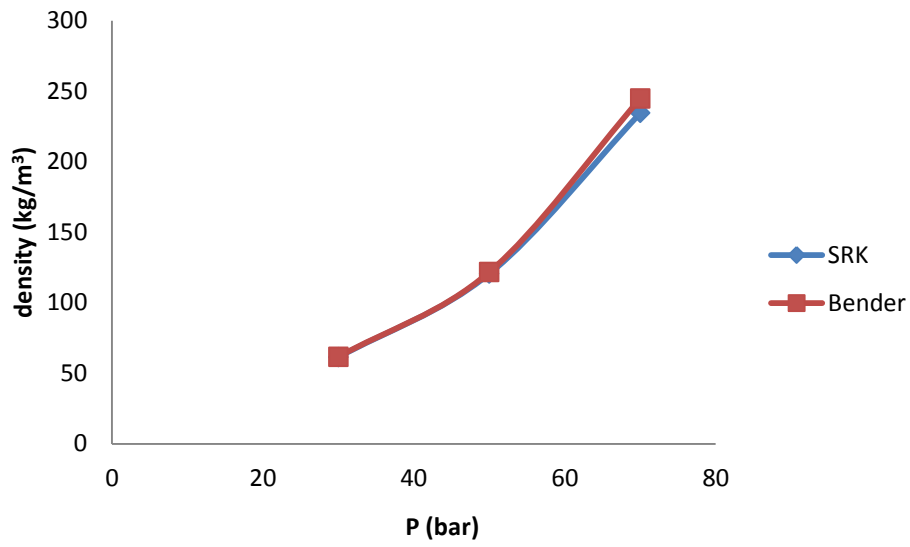


Figure 4.3: Carbon dioxide density at 34°C

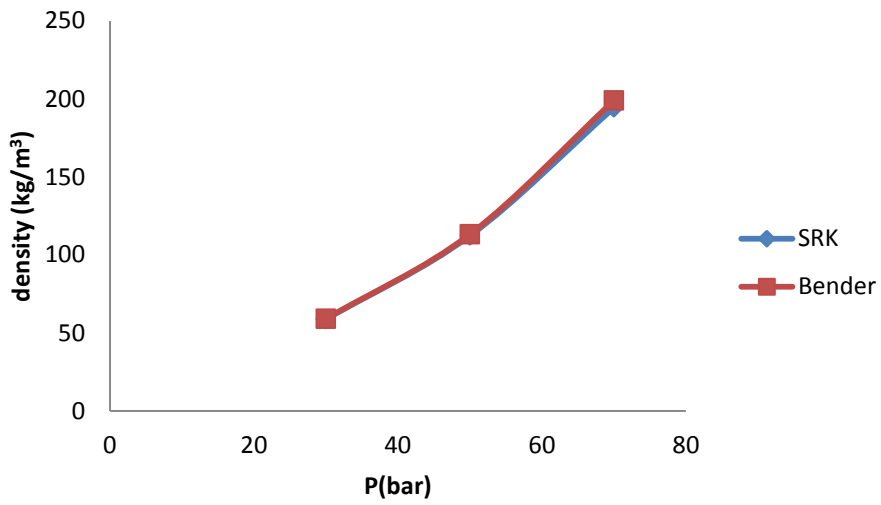


Figure 4.4: Carbon dioxide density at 40°C

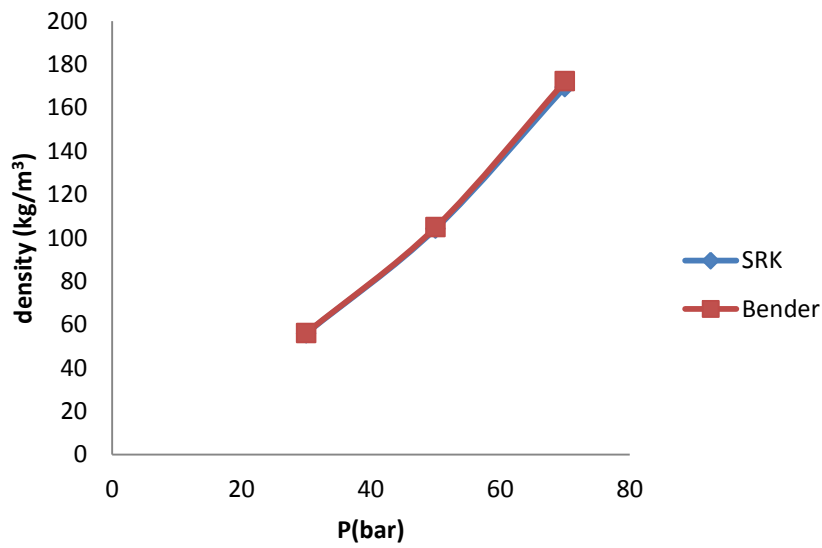


Figure 4.5: Carbon dioxide density at 50°C

Clearly, SRK seems to be reliable for the calculation of the carbon dioxide density, as shown in Figures 4.2, 4.3, 4.4 and 4.5.

Data of water solubility on CO₂ obtained with SRK in Aspen Plus have been compared to experimental data from literature (³⁸). The results are shown in Figure 4.6.

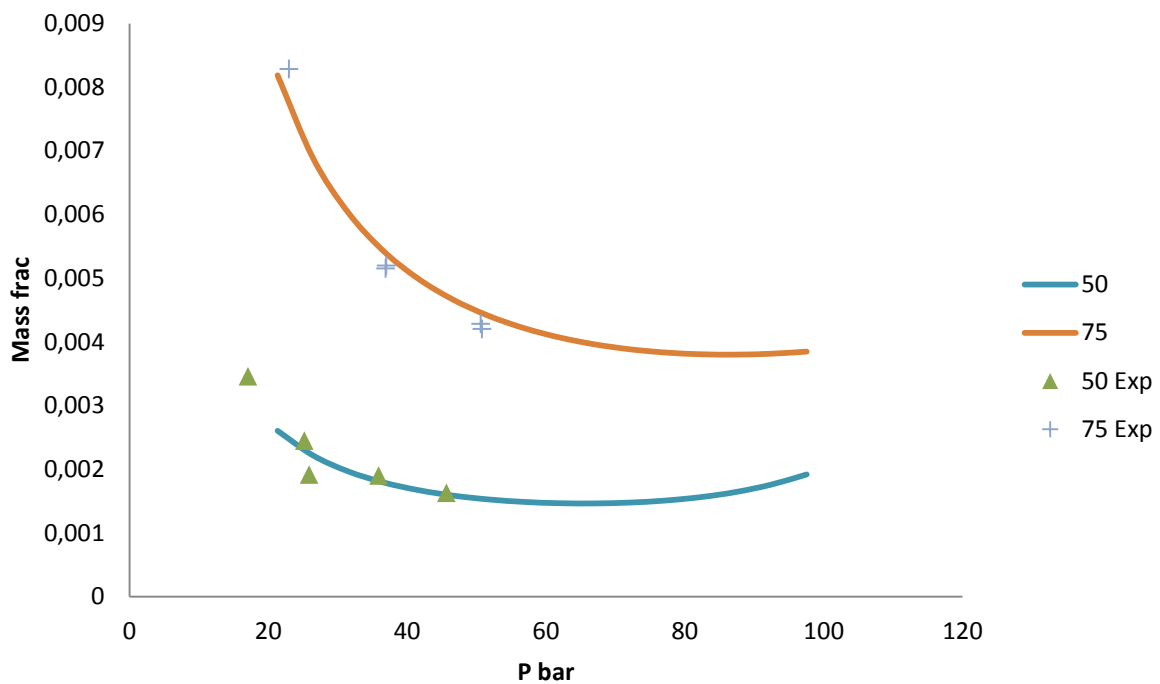


Figure 4.6: Water solubility in CO₂

Since even for water solubility experimental data and data calculated with SRK are similar, SRK is considered to be a reliable property method for our operating conditions.

The final flow sheet is reported in figure 4.7

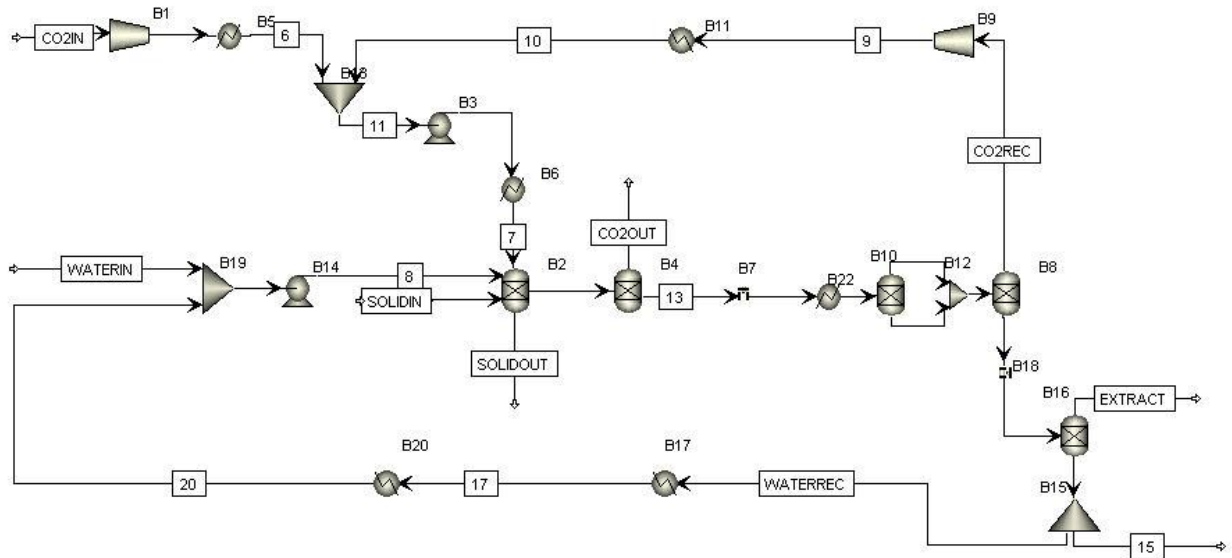


Figure 4.7: Aspen Plus flow sheet of the process

As shown in Figure 4.7, the carbon dioxide at atmospheric conditions is compressed at 60 bar (B1) and then cooled down to 5 °C (B5) to liquefy. Liquid carbon dioxide is pumped at the desired extraction pressure (B3) and heated up to the desired extraction temperature (B6) and goes to the extractor. Since there is not a “Supercritical Extractor block” available in Aspen Plus 7.3, a Sep block (B2) has been used. The supercritical solvent, added with the co-solvent and loaded with the extract is separated from the part that has not been extracted. An external calculator block (called “EXTRACTO”) has been used to calculate the split fraction of the oil component, according to the experimental curves (“k1” and “k2” parameter of the Fortran block). In the block B4, the carbon dioxide lost at the end of the extraction during the opening a refilling steps (while another extractor is operating in parallel) is separated. A calculator block (called “CO2 OUT”) calculates the flow of carbon dioxide lost. A valve (B7) is used for reducing the pressure at the desired separation pressure and a heat exchanger (B22) is used to reach the desired separation temperature. To simulate the separation unit, a Sep block (B8) is used. A calculator block (called “SEPARATO”) is used to calculate the split fraction of water and oil. In this block the solubility of oil calculated using the Chrastil equation, whose parameters have been calculated from the experimental data (4.2).

$$S = \rho^4 * e^{-\frac{14824}{T}} \quad (4.2)$$

Where S is the solubility (g/kg) of oil in CO_2 , ρ is the density (g/L), and T is the temperature of the block (K). For the calculation of density, the separation block B10 is used to separate CO_2 since the software can calculate the density of a stream, not of a component.

For the solubility of water a curve that interpolates experimental literature data ⁽³⁸⁾ is been used (4.3)

$$S_w = 1.66 * 10^{-9} + 7.36 * 10^{-8} * T + 4.54 * 10^{-8} * P + 1.22 * 10^{-6} * P * T \quad (4.3)$$

Where S_w is solubility of the water in CO_2 (kg/kg), P is the pressure (bar) of the block B7, T is the temperature ($^{\circ}\text{C}$) of the block B22. At optimal conditions 72 bar and 34 $^{\circ}\text{C}$, in the CO_2 recycling stream water is 0.297 wt % and oil in practice absent.

Carbon dioxide passes to gas phase after depressurization and is completely recovered, it is sent to the compressor (B9), that raises the pressure to 75 bar. At this pressure the temperature is decreased to 5 $^{\circ}\text{C}$ and allow the carbon dioxide to liquefy. Carbon dioxide is then sent to the pump (B3) to reach the extraction pressure.

After being separated from the CO_2 in the block B8, the extract has to be separated from water. The stream EXT is depressurized at atmospheric pressure by the valve B18 and sent to the water separator. To reproduce the laboratory conditions (rotavapor), this separation should be done by a crystallizer. A separation block (B16) is used to separate entirely water from the extract. To evaluate the duty that should be supplied to evaporate water and the duty to take out to condense water and recycle it, two heat exchangers have been used. Water is theoretically completely recycled, however for problem of convergence, a purge of 1% has been put in the split block B15. The water recycled is sent to the pump (B14) to reach the desired extraction pressure.

Three designed specifications have been set. The production was fixed at 30 kg/h of oil extract with the design specification called "PRODUCT": the flow rate of solid in was varied in order to keep this production constant. The inlet of carbon dioxide to extraction was fixed with the design specification "CO2REC", where the flow rate of carbon dioxide of stream 5 was fixed at 30000 kg/h varying the flow rate of fresh carbon dioxide of the stream "CO2IN". A similar design specification was fixed for water: the flow rate of water that enters to the extractor was fixed at the 7 % of that of carbon dioxide varying the flow rate of fresh water in "WATERIN". Another design specification (HEX2) was imposed to assign the temperature of the carbon dioxide separation block (B8). The temperature of the heat exchanger B22 was varied in order to keep the vapor fraction of the stream "CO2REC" at 1.

4.2 Economical analysis of the process

A calculator block (called “PRODCOST”) has been implemented to calculate the manufacturing cost. An operation time of 8760 h/year has been considered. The cost of hot utilities, cold utilities, electricity and raw materials have been calculated.

Prices of the utilities, that were took from Turton at al. 2009 (³⁹), are summarized in Table 4.2

Table 4.2: Utilities

	Cost (\$/GJ)	BLOCK
Common Utilities		
Electricity (110V - 440V)	16.8	B1,B3,B9,B14
Cooling Water (30°C to 45°C)	0.354	B18
Steam		
Low Pressure (5 barg, 160°C)	6.08	B6,B22,B17
Refrigeration		
Moderately Low (5°C)	4.43	B5, B11

The price of the raw materials considered are shown in Table 4.3

Table 4.3: Price of raw materials: rucola (⁴⁰), CO₂ and water(⁴¹).

	Price \$/kg
Rucola	0.75
CO ₂	0.279
Water	0.0014

In order to optimize the production cost, the effect of the separation pressure at different extraction pressures was analysed. The production cost has been calculated at the production of 30 kg/h. The results are shown in Figure 4.8.

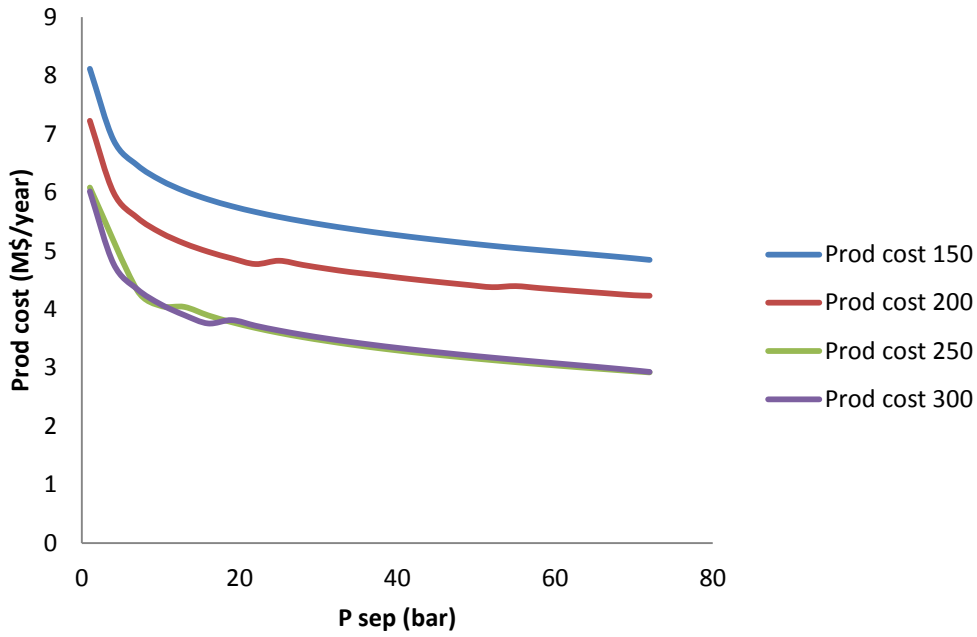


Figure 4.8: Production cost at different separation pressures at different extraction pressures

As can be seen, there is not a minimum value of the production cost. Increasing the separation pressure there is anyway a decreasing of the production cost, common to all the extraction pressures. So, the critical CO₂ pressure was set as maximum of this process. Accordingly, 72 bar was kept as the optimum separation pressure.

The effect of the extraction conditions on the production cost has been investigated. The production cost has been calculated at different extraction pressures. The results are shown in Figure 4.9.

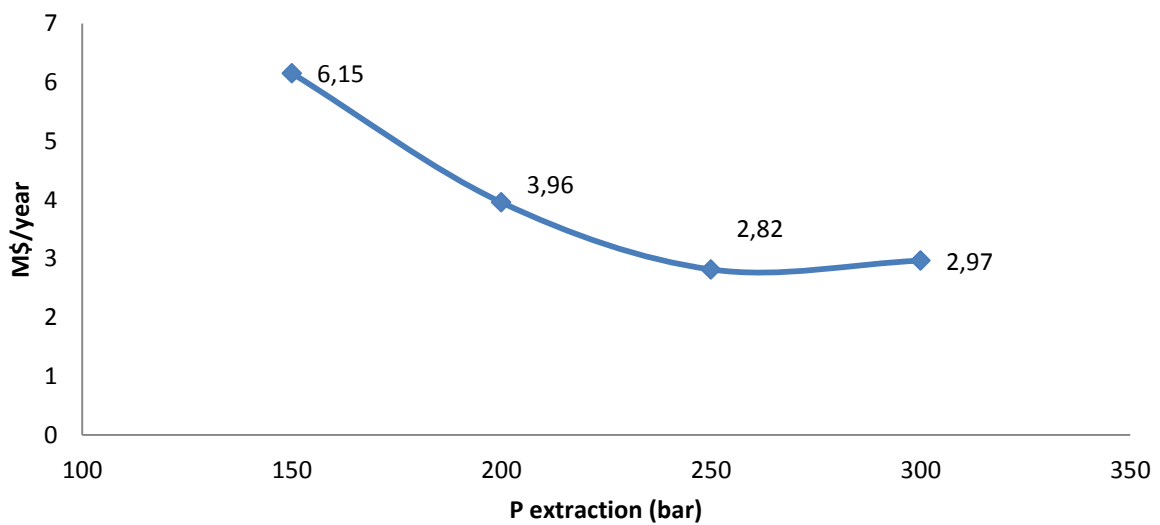


Figure 4.9: Production cost at different extraction pressures at 65°C

According to the Figure 4.9 there is an optimum value of the extraction pressure at 250 bar. The percentage distribution of the production cost at different extraction pressures is shown in Figure 4.10.

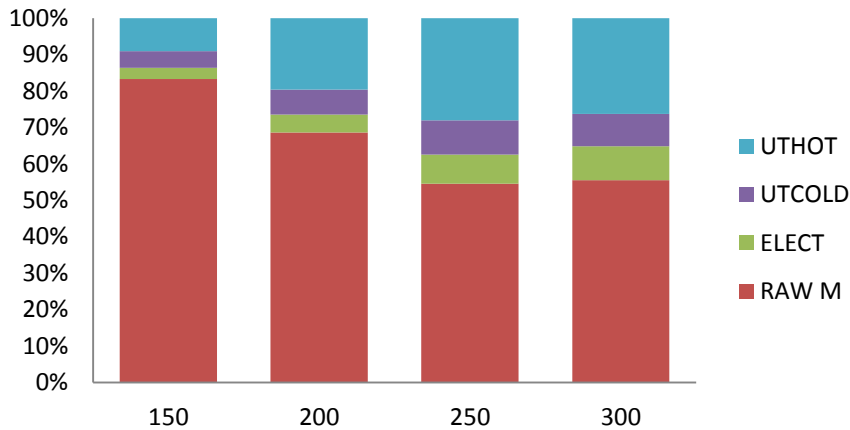


Figure 4.10: Production cost distribution at different extraction pressures

As can be seen raw materials effects more the cost in all cases. The pumping cost (ELECT) is lower at low extraction pressures and higher at 300 bar. The influence of the cost of utilities is higher at high extraction pressures.

The effect of the extraction temperature on the production cost has been investigated. The production cost has been calculated at different extraction temperatures at 300 bar, according to the experimental extraction curves. The results are shown in Figure 4.11

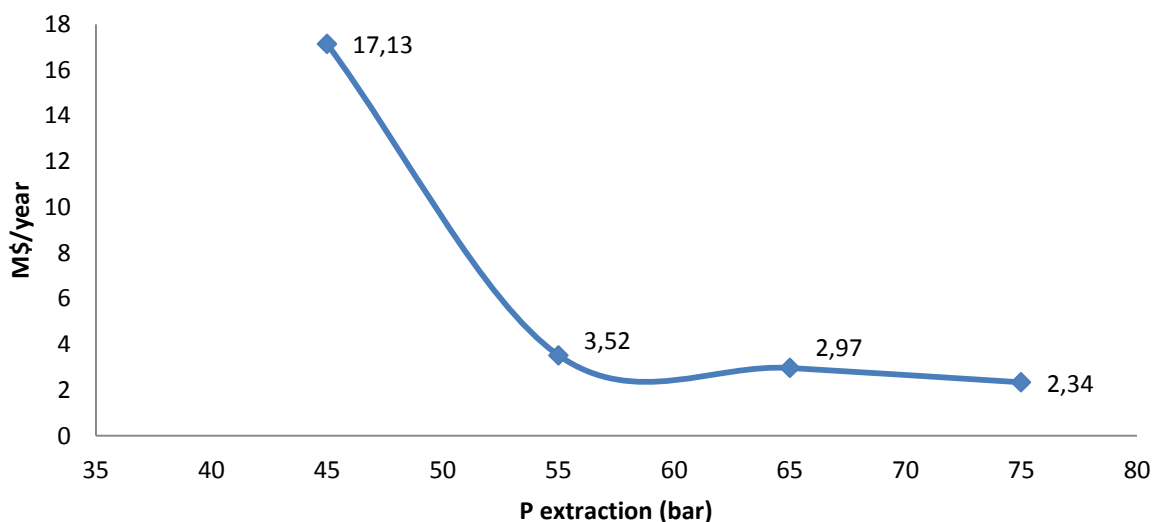


Figure 4.11: Production cost at different extraction temperatures at 300 bar.

Increasing of the extraction temperature has an effective impact in reducing the production cost passing from 45°C to 55°C. The production cost is lower at 65°C and lowest at 75 °C. The distribution of the production cost at different temperatures is shown in Figure 4.12.

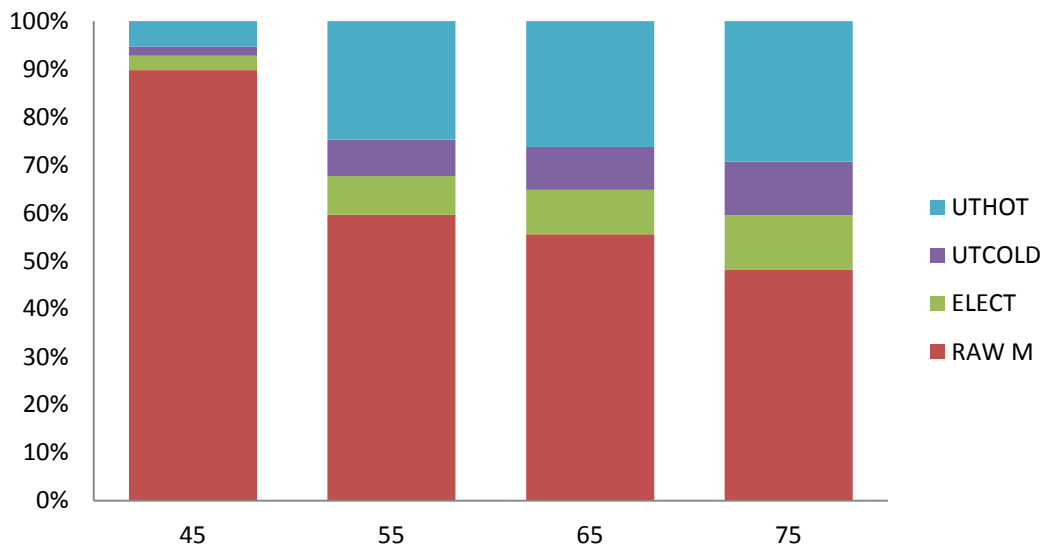


Figure 4.12: Distribution of the production cost at different extraction temperatures.

As can be clearly seen, what effects more the cost are raw materials in all cases. Since the yield of extraction at lower temperature is lower, consumption of raw materials increases leading to an enhancement of the total production cost.

The influence of the flow rate of recycle of carbon dioxide on the production cost has also been calculated. The production cost has been calculated at 300 bar and 65 °C of extraction at different carbon dioxide recycle flow rates. The results are shown in Figure 4.13.

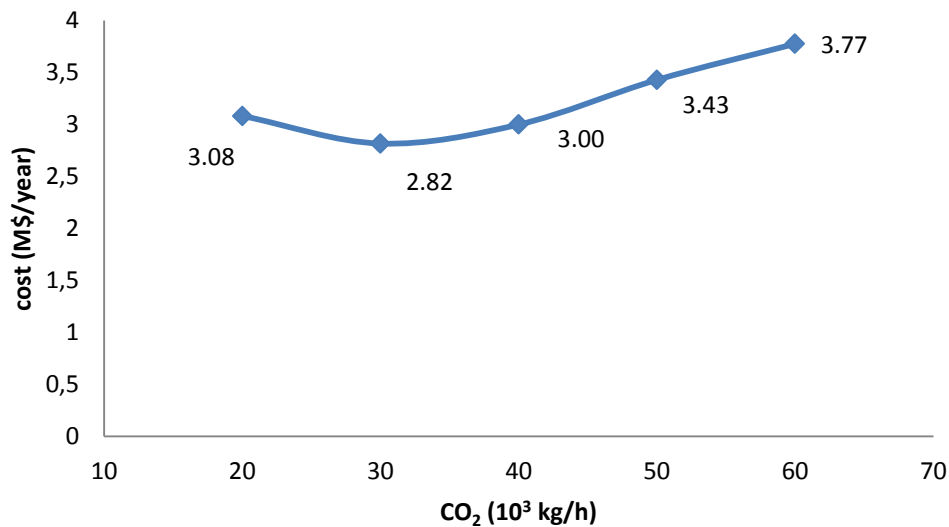


Figure 4.13: Production cost at different CO₂ flow rates

Figure 4.13 shows that an optimum value is around 30000 kg/h.

The equipment costs have been calculated for the flow sheet at optimum conditions (extraction at 250 bar and 65 °C , separation at 72 bar, flow rate of carbon dioxide 30000

kg/h) using formulas suggested by Douglas (36). Aspen plus evaluation option was used for sizing of the equipment (except for the extractors). For heat exchangers, the equation 4.3 has been applied.

$$\text{Cins US\$} = \frac{M\&S}{280} * 101.3 * A^{0.65} * 2.29 + Fc \quad (4.3)$$

Where $M\&S$ is the Marshall & S wift index considered 1469.6 (0.2% year from 1457.4 of 2010), A is the exchange area (ft²) and Fc is a corrective value.

For the each vessel, the equation 4.4 has been used.

$$\text{IC reactor US\$} = \frac{M\&S}{280} * 101 * D_R^{1.066} * L_R^{0.802} * 2.18 + Fc \quad (4.4)$$

Where D_R is the diameter (ft) and L_R is the length of the vessel. For the compressors, the equation 4.5 has been applied.

$$\text{IC Comp US\$} = \frac{M\&S}{280} * 517.5 * bhp^{0.82} * 2.11 + Fc \quad (4.5)$$

Where bhp is the brake power (hp). Fc is 1.55 for the extractor vessels and 1.52 for the rest of the equipment.

The results obtained after calculating the equipment costs are shown in Table 4.4.

Table 4.4: Total equipment cost

Equipment	\$
Heat exchangers	336064
Vessels (3 extractors + 1 flash vessel)	66408
Compressors	426893
Total equipment cost	829366

The distribution of the equipment cost is shown in Figure 4.14.

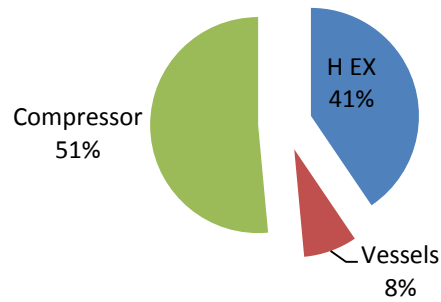


Figure 4.14: Equipment cost distribution

The total production cost distribution is shown in Figure 4.15. The equipment cost are annualized according to Douglas (³⁶), using a capital charge factor (CCF) equal to 1/3. The figure shows that the fixed capital (FCI) is really small compared to the production cost. Raw materials are the most expensive production cost (50%). Hot utilities (UTHOT) effects more the production cost than cold utilities (UTCOLD), while the influence of pumping is lower (ELECT).

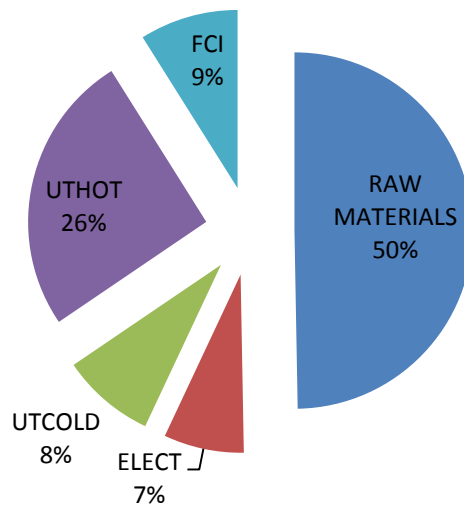


Figure 4.15: Total manufacturing cost distribution.

Finally, an analysis of the profitability of the process has been made. The total capital investement (TCI) and the total production cost (TPC) have been estimated using the formula of Douglas (³⁶), shown in equations 4.6 and 4.7.

$$TCI (\$) = 2.36 \text{ Direct costs onsite} \tag{4.6}$$

$$TPC \frac{\$}{year} = 1.03 * raw\ materials + utilities + 0.186\ direct\ costs\ onsite + 2.13 * 10^5\ n^{\circ}operatoras + 0.025\ incoming \quad (4.7)$$

The total capital investment and the total production cost are shown in Table 4.5

Table 4.5: Estimate of TCI and TPC

	\$ / year
TCI	1957304
TPC	6079304

For the evaluation of the profitability the following hypothesis has been considered :

- Life of the plant =10 years
- Period of start up = 2 years
- Depreciation = (DDB method)7 years
- Taxation = 40 %
- Interest = 10%
- Fixed capital land = 1000000 \$
- Residual value = 150000\$

The market price of the extract varies from 10 to 80 \$/kg (⁴²). With the hypothesis considered the process will have a net present value positive at the end of life if the price of the extract is higher than 29.8 \$/kg. The flow cash diagram is shown in Figure 4.16.

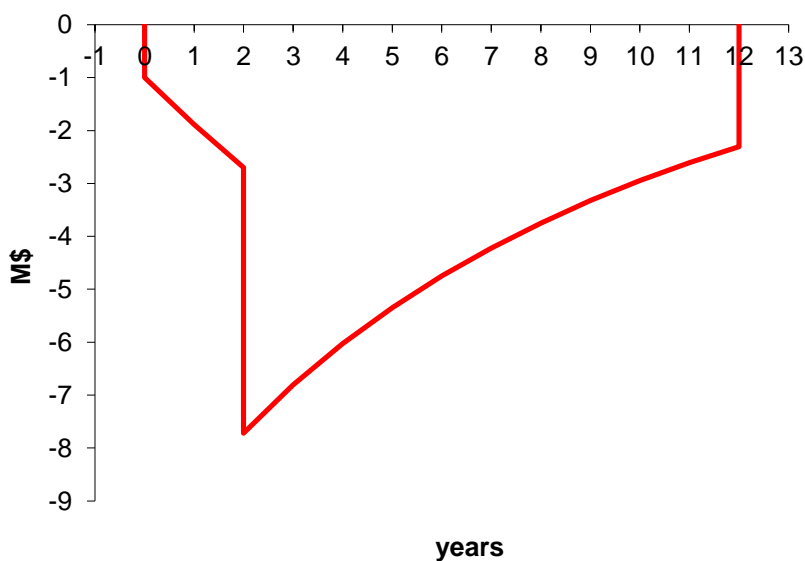


Figure 4.16: Cash Flow diagram

Since the process is profitable if the selling price of the extract is higher than 29.8\$/kg and since the market price can be much bigger (80\$/kg), this process can be interesting for future developments.

Conclusion

Different experimental tests have been carried out in order to extract glucosinolates, flavonoids and fatty acids from leaves of rocket salad (*Eruca sativa*) using supercritical carbon dioxide extraction. SC-CO₂ extractions using pure CO₂ and three co-solvents (water, ethanol and methanol) have been carried out. Results show that SC-CO₂ extraction is faster and available at lower temperatures compared to the Soxhlet. When ethanol was employed as co-solvent, the best yield (5.54 %) was obtained at 300 bar, 65 °C, 0.5 mL/min of ethanol and 0.3 kg/h of carbon dioxide. Applying a mechanical pre-treatment was observed to increase the yield. Then, SC-CO₂ was performed using water as co-solvent and the influence of the extraction variables was investigated. The optimum values of water dosage and temperature were 0.4 mL/min and 65°C, respectively. Increasing of temperature was observed to have a direct effect on the enhancement of the extraction yield, while increasing of pressure did not effect significantly the extraction yield. Comparing ethanol, methanol and water at the same extraction conditions (300 bar, 45°C and 7 wt % co-solvent), the yield obtained with ethanol and methanol were similar (5.54 and 5.56 %, respectively) while the yield obtained with water was much higher (21.71 %). The analysis of the extract shows that glucosinolates and flavonoids were mainly extracted using water as co-solvent. The highest amount of glucosinolates was obtained with 0.4 mL/min of water at 300 bar, glucoraphanin and DMB-GLS were the main compounds. The highest amount of flavonoids was obtained with 0.4 mL/min of water at 300 bar at the highest temperature (75 °C), Quercetin derivatives were the main compounds. Glucosinolates and flavonoids were extracted using SC-CO₂ while only traces of them have been found in the Soxhelt extracts. Lipids were extracted using pure SC-CO₂, being the extract very rich in unsaturated fatty acids.

A conceptual design of an industrial process that produces an extract rich in glucosinolates and flavonoids starting from freeze-dried rocket salad, water and carbon dioxide has been proposed. The basic idea was a scale-up of the laboratory plant to a size able to treat 100 kg/h of rocket salad. The software Aspen Plus has been employed for the simulation. The influence of the extraction pressure and the extraction temperature has been investigated, obtaining the lowest production cost at 250 bar and 65 °C. The effect of the separation pressure on the production cost has also been studied, obtaining an optimum value at 72 bar. Finally, an analysis of the profitability of the process was made showing that with an interest of 10% the net present value of the process would be positive if the selling price of the extract was higher than 29.8 \$/kg.

References

1. Eggers R , Pilz S (2011), High Pressure Processing, *Industrial Scale Natural Products Extraction*, Wiley-VCH Verlag GmbH & Co. KGaA.
2. Brunner G (2004), Supercritical fluids: technology and application to food processing. *Journal of Food Engineering*, 67, 21-33.
3. "Phase change data for Carbon dioxide". National Institute of Standards and Technology. Retrieved 2008-01-21.
4. Beckman EJ (2003), Supercritical and near-critical CO₂ in chemical synthesis and processing, *Journal of Supercritical Fluids*, 28, 121-191.
5. Praxair Material Data safety sheet, P-4574-H, May, 1999.
6. Yaniv Z (1997), Traditions, uses and research on rocket in Israel, *Rocket, a Mediterranean crop for the world*, International Plant Genetic Institute, Rome, 76-80.
7. Alqasoumi S, Al-Sohaibani M, Al-Howiriny T, Al-Yahya M, Rafatullah S.(2009), Rocket "*Eruca sativa* ": A salad herb with potential gastric anti-ulcer activity. *World J Gastroenterol* ; 15(16): 1958-1965 .
8. Lynn A, Collins A, Fuller Z, Hillman K, Ratcliffe B (2006). Cruciferous vegetables and colo-rectal cancer. *Proc. Nutr. Soc.*, 65: 135-144.
9. Rafatullah S, AlSheikh A, Alqasoumi S, Al-Yahya M, El-Tahir K, Galal A (2008). Protective effect of fresh radish juice (*Raphanus sativus* L.) against carbon tetrachloride induced hepatotoxicity. *Int. J. Pharmacol.*, 4: 1-5.
10. Pasini F Verardo, Caboni V MF, D'Antuono LF (2012), Determination of glucosinolates and phenolic compounds in rocket salad by HPLC-DAD-MS: Evaluation of *Eruca sativa* Mill. and *Diplotaxis tenuifolia* L. genetic resources. *Food Chem.* 133, 1025–1033.
11. Douglas C, Abbel S (2006), Glucosinolate metabolism and its control, *Plant Science*, Vol.11 No.2.
12. Shroff R, Vergara F, Muck A, Savatos A, Gershenzon J (2008), Nonuniform distribution of glucosinolates in *Arabidopsis thaliana* leaves has important consequences for plant defense, *PNAS*, Vol.105 No.16.
13. Das S, Tyagi A K, Kaur H (2000). Cancer modulation by glucosinolates: a review. *Current Science*, 79(12), 1665–1671.
14. Keum YS, Jeong WS, Kong ANT(2004), Chemoprevention by isothiocyanates and their underlying molecular signalling mechanisms,*Mutation Research*, 555, 191–202.
15. Smith TJ (2001), Mechanisms of carcinogenesis inhibition by isothiocyanates, *Expert Opinion on Investigational Drugs*, 10, 2167–2174.

16. Zhang Y (2004), Cancer-preventive isothiocyanates: Measurement of human exposure and mechanism of action, *Mutation Research*, 555, 173–190.
17. Bennett RN, Mellon FA, Botting NP, Eagles J, Rosa EAS, Williamson G (2002). Identification of the major glucosinolate (4-mercaptobutylglucosinolate) in leaves of *Eruca sativa* L., *Phytochemistry*, 61, 25–30.
18. Kim SJ, Jin S, Ishii G. (2004), Isolation and structural elucidation of 4-(β -D-glucopyranosyl)butyl glucosinolate from leaves of rocket salad (*Eruca sativa* L.) and its antioxidative activity, *Bioscience Biotechnology Biochemistry*, 68, 2444–2450.
19. Daxenbichler ME, Spencer GF, Carlson DG, Rose GB, Brinker AM, Powell RG (1991), Glucosinolate composition of seeds from 297 species of wild plants, *Phytochemistry*, 30, 2623–2638.
20. Cataldi TR, Rubino A, Lelario F, Bufo SA (2007), Naturally occurring glucosinolates in plant extracts of rocket salad (*Eruca sativa* L.) identified by liquid chromatography coupled with negative ion electrospray ionization and quadrupole ion-trap mass spectrometry, *Rapid Communication in Mass Spectrometry*, 21, 2374–2388.
21. Erlund I (2004), Review of the flavonoids quercetin, hesperetin, and naringenin. Dietary sources, bioactivities, bioavailability, and epidemiology. *Nutrition Research*, 24, 851–874.
22. Halliwell B, Zhao K, Whiteman M (2000). The gastrointestinal tract: A major site of antioxidant action, *Free Radical Research*, 33, 819–830.
23. Ko MJ, Cheigh CI, Cho SW, Chung MS (2014). Relationship analysis between flavonoids structure and subcritical water extraction (SWE), *Food Chemistry*, 143, 147–155.
24. Sun M, Xu L, Saldana MDA, Temelli F (2008), Comparison of canola meals obtained with conventional methods and supercritical CO₂ with and without ethanol, *Journal of Oil Chemistry Soc*, 85, 667–675.
25. Liza MS, Abdul Rahman R, Mandana B, Jinap S, Rahmat A, Zaidul ISM, Hamid A (2010), Supercritical carbon dioxide extraction of bioactive flavonoid from *Strobilanthes crispus* (Pecah Kaca), *Food and Bioprocess Technology*, 88, 319–326.
26. Gamache PH, McCabe D, Parvez H, Parvez S and Acworth IN, 1997. *Progress in HPLC-HPCE*, vol. 6, VS Press, The Netherlands, 99–126.
27. Abu BMF, Teh AH, Rahmat A, Osman F (2006), Effects of *Strobilanthes crispus* tea aqueous extracts on glucose and lipid profile in normal and streptozotocin-induced hyperglycemic rat. *Plant Foods Hum Nutr*, 61(1), 7–12.
28. Chiu KL, Cheng YC, Chen JH, Chang CJ, Yang PW (2002), Supercritical fluids extraction of *Ginkgo ginkgolides* and flavonoids, *Journal of Supercritical Fluids*, 24, 77–87.

29. Arnaiz E, Bernal J, Martin MT, Garcia-Viguera C, Bernal JL, Toriblo L (2011), *Journal of Lipid Science Technology*, 113, 479-486.
30. http://www.inran.it/646/tabelle_di_composizione_degli_alimenti.html?idalimento=005460&quant=100.
31. <http://www.ellab.com/applications/medical/pharma/lyophilization.aspx>.
32. Bertucco A, Vetter G (2001), Supercritical fluid extraction and fractionation from solid materials, *High pressure process technology: Fundamentals and applications*, Elsevier, 378-379.
33. Bertucco A, Vetter G (2001), Supercritical fluid extraction and fractionation from solid materials, *High pressure process technology: Fundamentals and applications*, Elsevier, 387-388.
34. Da Porto C, Natolino A, Decorti D (2014), Extraction of proanthocyanidins from grape marc by supercritical fluid extraction using CO₂ as solvent and ethanol-water mixture as co-solvent, *Journal of supercritical fluids*, 16, 1-8.
35. <http://goldbook.iupac.org/D01751.html>
36. Douglas JM (1988), *Conceptual design of Chemical Processes*, McGraw-Hill, New York (USA).
37. Bender E, Equations of state exactly representing the phase behavior of pure substances, in: *Proceedings of the Fifth Symposium on Thermophys. Prop.*, ASME, New York, 1970.
38. Coan RC, King AD (1971), Solubility of Water in Compressed Carbon Dioxide, Nitrous Oxide, and Ethane. Evidence for Hydration of Carbon Dioxide and Nitrous Oxide in the Gas Phase, *Journal of the American Chemical Society*, 93, 1857.
39. Turton R (2009), *Analysis, synthesis, and design of chemical processes*, 3rd ed, Upper Saddle River, N.J. : Prentice Hall.
40. <http://www.an.camcom.gov.it/sites/default/files/Listino%20febbraio%202012.pdf>
41. <http://www.icis.com/>
42. <http://www.alibaba.com/>